Journal of Medicinal Chemistry

pubs.acs.org/jmc Article

Novel Functionalized Cannabinoid Receptor Probes: Development of Exceptionally Potent Agonists

Shan Jiang,[#] Christos Iliopoulos-Tsoutsouvas,[#] Fei Tong, Christina A. Brust, Catherine M. Keenan, Jimit Girish Raghav, Tian Hua, Simiao Wu, Jo-Hao Ho, Yiran Wu, Travis W. Grim, Nikolai Zvonok, Ganesh A. Thakur, Zhi-Jie Liu, Keith A. Sharkey, Laura M. Bohn, Spyros P. Nikas,* and Alexandros Makriyannis*

Cite This: *J. Med. Chem.* 2021, 64, 3870−3884 Read Online

ACCESS | Metrics & More | Article Recommendations | Supporting Information

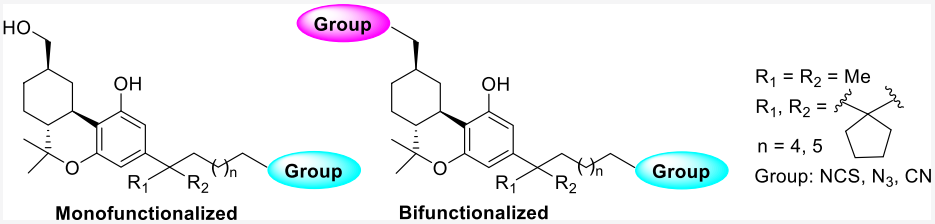

ABSTRACT: We report the development of novel cannabinergic probes that can stabilize the cannabinoid receptors (CBRs) through tight binding interactions. Ligand design involves the introduction of select groups at a judiciously chosen position within the classical hexahydrocannabinol template (monofunctionalized probes). Such groups include the electrophilic isothiocyanato, the photoactivatable azido, and the polar cyano moieties. These groups can also be combined to produce bifunctionalized probes potentially capable of interacting at two distinct sites within the CBR-binding domains. These novel compounds display remarkably high binding affinities for CBRs and are exceptionally potent agonists. A key ligand (**27a**, AM11245) exhibits exceptionally high potency in both *in vitro* and *in vivo* assays and was designated as "megagonist," a property attributed to its tight binding profile. By acting both centrally and peripherally, **27a** distinguishes itself from our previously reported "megagonist" AM841, whose functions are restricted to the periphery.

INTRODUCTION

The two $G_{i/o}$-protein-coupled cannabinoid receptors (CBRs) CB1 and CB2 have been recognized as important therapeutic targets for CNS[1] and cardiometabolic[2] disorders, glaucoma,[3] pain,[4] cancer,[5] as well as conditions related to the immune system.[6] An interesting feature of these two GPCRs is their ability to be modulated by several structurally distinct classes of compounds including endogenous lipid-like substances (*e.g.*, anandamide and 2-arachidonoyl glycerol), as well as exogenous synthetic (*e.g.*, nabilone and rimonabant) and plant-derived molecules [e.g., (−)-Δ^9-tetrahydrocannabinol].[7] For the cannabinoid CB1 receptor, such ability to respond to a plethora of ligands of considerably different sizes and shapes is consistent with the remarkable plasticity of its orthosteric binding pocket, as revealed by studies on the agonist- and antagonist-bound crystal structures,[8,9] as well as the cryo-electron microscopy (cryo-EM) structures of agonist-bound CB1 in complex with G_i.[10,11] Furthermore, the ligand-dependent activation of CB1 and CB2 is multifactorial and can activate distinctly different signal transduction pathways [e.g., G proteins (canonical $G\alpha_{i/o}$ or non-canonical $G\alpha_s$, $G\alpha_{16}$, and $G\alpha_{q/11}$) *vs* arrestins].[12,13] This phenomenon is more general in GPCRs, and it is referred to as "functional selectivity" or "ligand bias.".[14,15] Functional selectivity derives from a ligand-dependent stabilization of a receptor's conformation that favors interactions with an intracellular protein at the expense of others among the possible active receptor conformations. Additionally, the ligand−receptor binding kinetics have emerged as an important concept in GPCR drug development as they may influence the functional potency and efficacy of both agonists and antagonists.[16,17] Different ligands for a GPCR may have distinct association and dissociation kinetics which determine the residence time of the ligand on the receptor. Ligands with significantly slow dissociation in a non-equilibrium system exhibit pseudo-irreversible binding properties.[18] In the case of CB1, we have observed such effects with a ligand exhibiting irreversible binding characteristics for the receptor. We designated this

Received: November 25, 2020
Published: March 24, 2021

https://dx.doi.org/10.1021/acs.jmedchem.0c02053
J. Med. Chem. 2021, 64, 3870−3884

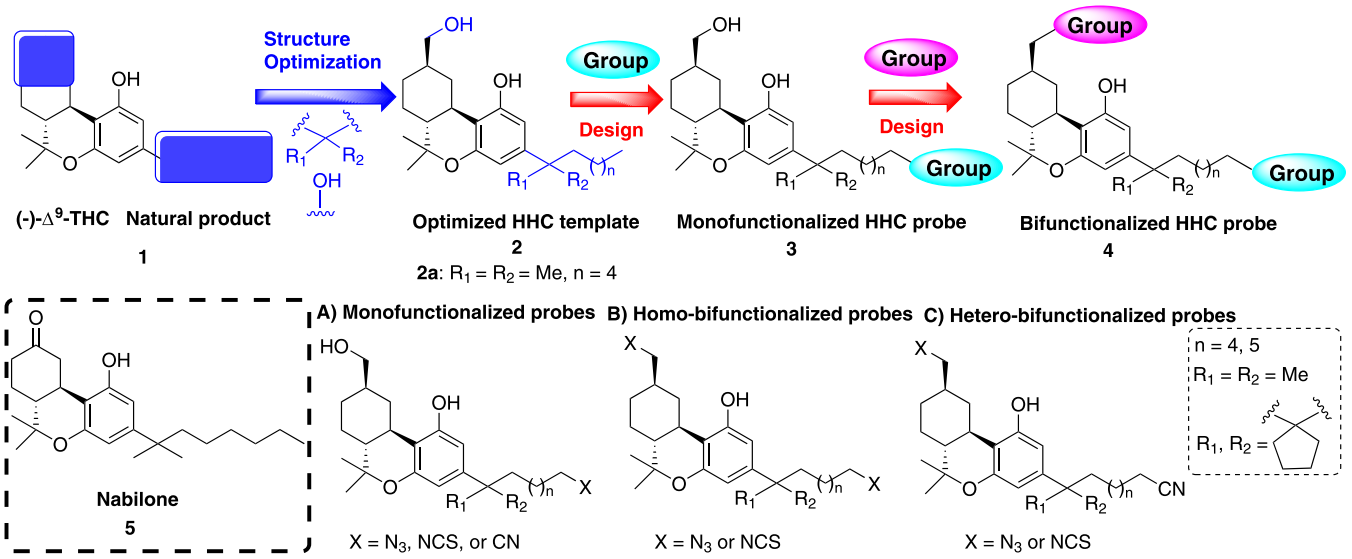

Figure 1. Design of the novel mono and bifunctionalized HHC probes and structures of the natural product (−)-Δ^9-THC and the marketed HHC drug nabilone.

exceedingly potent agonist as "megagonist."[19,20] Moreover, the lifetime of the ligand−receptor complex may also determine its preferential signaling mechanisms and lead to functional selectivity.[21]

Deeper understanding of the molecular basis of the ligand−CBR binding motif(s) and the kinetics through which ligands block or enable signaling events and intracellular processes offers the opportunity to develop more targeted cannabinoid-based therapeutics. Toward this goal, our laboratory has developed the ligand-assisted protein structure (LAPS), a successful approach that is currently being used to explore the binding motif(s) of cannabinergic ligands with their respective native receptors with a focus on exploring how these motifs are associated with distinct signaling profiles.[22,23] LAPS is a powerful tool that utilizes a combination of purpose-designed cannabinergic ligands, CBR mutants, and mass spectrometric proteomic analysis and allows for the characterization of critical receptor residues that interact with a chemically and functionally diverse set of ligands at the level of specific amino acid residues.[20,24−28] Design of such ligands is based on the incorporation of reactive groups at carefully chosen sites within the chemical structure of interest. The reactive groups, we have generally chosen, include the electrophilic isothiocyanato and the photoactivatable azido moieties.[29,30] Over the past two decades, our laboratory has developed such ligands that represent different classes of cannabinergic compounds including endogenous, plant-derived, and synthetic agonists and antagonists at CB1 and CB2. These ligands allow us to identify amino acid residues within or near the binding pocket of the native receptor that are critical for ligand engagement and receptor function.[20,22−28,31−33] They have also been used to structurally characterize in more detail the CBR−ligand and CBR−G_i−ligand complexes using X-ray crystallography and cryo-EM, respectively.[8,9,11]

A considerable amount of our effort has been centered around the tricyclic hexahydrocannabinol (HHC) prototype, a chemical scaffold that: (a) exhibits the highest binding affinities for CB1/CB2 and the most potent *in vitro* and *in vivo* agonist properties, (b) encompasses three chiral centers, thus reducing target promiscuity, and (c) resembles the chemical structures of the marketed drugs THC and nabilone.[7,34] One of the analogues developed in this project, namely AM841,[30] has distinguished itself by being a valuable probe for LAPS studies,[20,28,30,31] a unique ligand for structural studies with the hCB1 receptor using X-ray crystallography and cryo-EM[8,11] and a peripherally acting cannabinergic "megagonist."[19,20] We have also extended the scope of the groups used in LAPS by adding moieties that may allow for the fine-tuning of the ligand's residence time within the receptors' site. One such group is the cyano moiety that albeit not being covalently active, it can develop polar and/or hydrogen bonding interactions with amino acid residues. Here, we report the design, synthesis, and biochemical and pharmacological characterization of novel HHC probes for the CBRs. Our key ligand AM11245 (**27a**) exhibits tight binding properties and exceptionally high potency in inhibiting the forskolin-stimulated cAMP accumulation and in various *in vivo* assays and was designated as "megagonist." Unlike the peripherally restricted "megagonist" AM841, AM11245 exhibited its "megagonist" profile both centrally and peripherally when tested *in vivo*.

RESULTS AND DISCUSSION

Design. Structure−activity relationship studies from our own and other laboratories have suggested that presence of *gem*-dimethyl or cyclopentyl groups at the C1′-position of the classical cannabinoids (HHC, or Δ^9/Δ^8-THC, **2**, **1**, Figure 1) enhances the ligand's potency and efficacy.[7,35−37] It has also been demonstrated that incorporation of various groups including heterocyclic rings at the ω-position of the side chain can maintain, or even enhance, the affinity of the compound for CBRs.[37−40] Additionally, in the classical cannabinoids, side chains consisting of six to eight linear methylene groups are optimal for activity.[7,36,39] Furthermore, it has been demonstrated in both HHCs and THCs that the presence of a hydroxyl at the northern region of the tricyclic prototype enhances the ligand's affinity for both CBRs.[7,37,41,42] Finally, we have shown that the presence of an equatorial hydroxymethyl group at C9 is optimal for activity.[43,44]

https://dx.doi.org/10.1021/acs.jmedchem.0c02053
J. Med. Chem. 2021, 64, 3870−3884

Scheme 1[a]

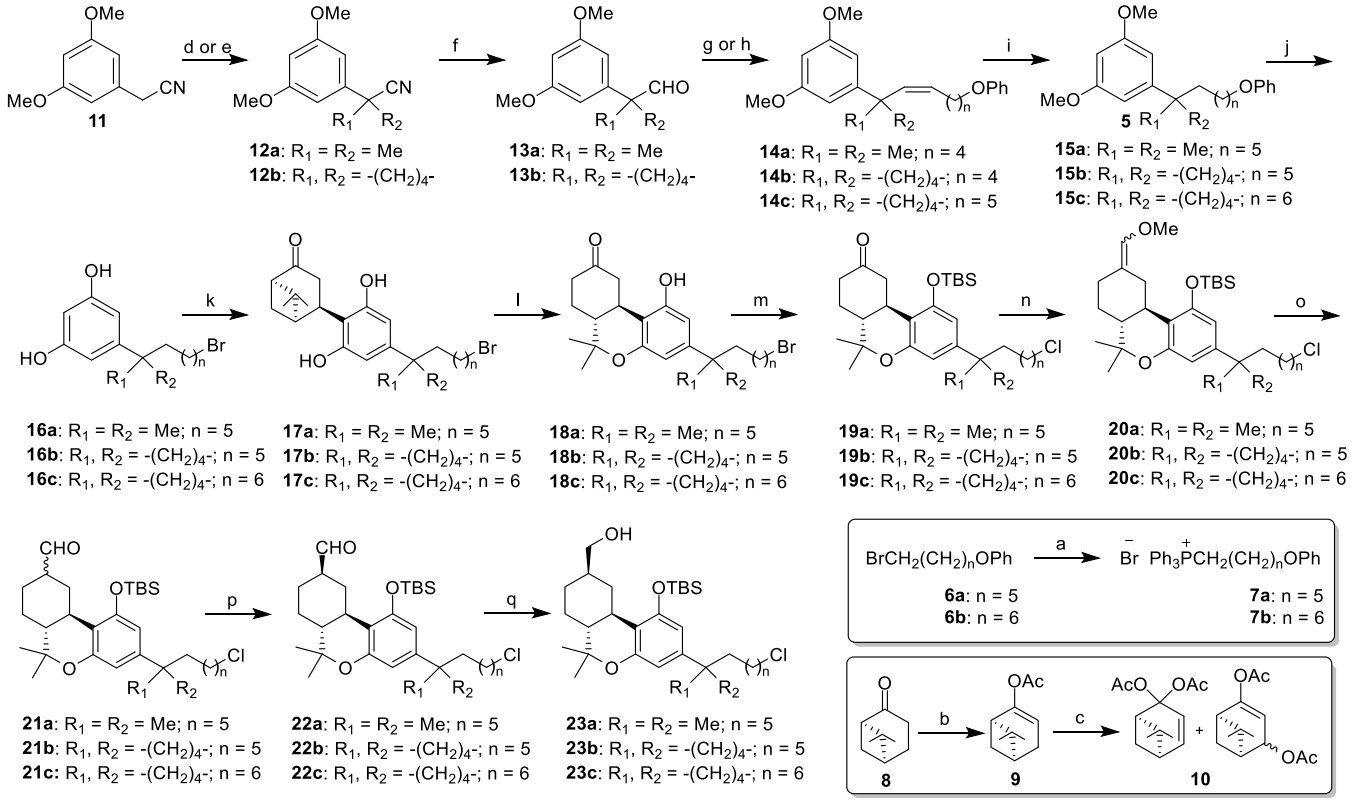

[a]Reagents and conditions: (a) PPh_3, benzene, reflux, 72 h, 98−99%; (b) isopropenyl acetate, *p*-toluenesulfonic acid, reflux, 6 h, 98%; (c) $Pb(OAc)_4$, benzene, reflux, 3 h; 90%; (d) CH_3I, NaH, DMF, 0 °C to r t, 2 h, 98%; (e) $(Me_3Si)_2N^-K^+$, $Br(CH_2)_4Br$, THF, 0 °C to r t, 5 min, 95%; (f) DIBAL-H, CH_2Cl_2, −78 °C, 0.5 h, 92%; (g) $Br^-P^+Ph_3(CH_2)_5OPh$, KHMDS, THF, 0−10 °C, 30 min, then addition of **13a** or **13b**, 0 °C to r t, 20 min, 96% for **14a** or 97% for **14b**; (h) $Br^-P^+Ph_3(CH_2)_6OPh$, KHMDS, THF, 0−10 °C, 30 min, then addition of **13b**, 0 °C to r t, 20 min, 96% for **14c**; (i) H_2, 10% Pd on C, AcOEt, r t, 2.5 h, 98%; (j) BBr_3, CH_2Cl_2, −78 °C to r t, 3 h, 91−92%; (k) **10**, *p*-TsOH, $CHCl_3$, 0 °C to r t, 4 days, 59−64%; (l) TMSOTf, CH_2Cl_2/$MeNO_2$, 0 °C to r t, 3 h, 70−75%; (m) TBSCl, imidazole, DMAP, DMF, 62 °C, 12 h, 91−93%; (n) $Cl^-Ph_3P^+CH_2OMe$, KHMDS, THF, 0 °C to r t, 1 h, then addition to **19a−c**, 0 °C to r t, 1.5 h, 70−73%; (o) Cl_3CCOOH, CH_2Cl_2, r t, 50 min, 90−95%; (p) K_2CO_3, EtOH, r t, 3 h, 80−84%; (q) $NaBH_4$, EtOH, 0 °C, 30 min, 97−98%.

Based on the above, our probe design adopts the 11-hydroxyl-HHC scaffold (**2**) with a seven or eight carbon long side-chain carrying a *gem*-dimethyl or a cyclopentyl substituent at the C1′. The site in which the reactive groups (−N_3, −NCS) are introduced is critical so that the ligands can optimally interact with the amino acid residue(s) within the receptor's binding domains.[7,23,27] Thus, incorporation of a reactive group at the *ω*-position of the side chain led to monofunctionalized probes (**3**) and the addition of a second reactive group at the C11 generated the bifunctionalized ligands (**4**). In addition to the C1′-*gem*-dimethyl-substituted bifunctionalized probes that we reported earlier,[28] we chose to explore the C1′-cyclopentyl-substituted HHCs in an effort to further refine the stability of the ligand−receptor complex. We also explored the potential of the cyano group at the *ω*-position of the side chain for its tight binding capability as this polar group is eight times smaller than a methyl group and, as reported, can develop polar interactions or hydrogen bonds with polar amino acid residues (*e.g.*, serine or arginine) in sterically congested environments.[45]

Chemistry. The monofunctionalized and the respective homo- and hetero-bifunctionalized probes for each series of analogues were prepared from a common advanced intermediate chloride (**23a−c**, Scheme 1). It is worth noting that the robustness of the multistep stereoselective approach is that which produces the final compounds in substantial quantities as required for subsequent *in vitro*, *in vivo*, and structural studies. For example, the synthesis of the key intermediate chlorides **23a−c** was accomplished in excellent overall yields (15−22%), and it requires 12 synthetic steps starting from commercially available **11**.

The optimized syntheses of the key intermediate chlorides **23a−c** are summarized in Scheme 1. Thus, deprotonation of **11** with sodium hydride followed by geminal dimethylation using methyl iodide gave nitrile **12a** (98% yield).[46] Sequential treatment of **11** with KHMDS and 1,4-dibromobutane afforded (3,5-dimethoxyphenyl) cyclopentane carbonitrile **12b** in very good yield (95%).[35] Reduction of the cyano group in **12a** and **12b** with diisobutylaluminum hydride led to the respective aldehydes **13a** and **13b** (92%) which upon Wittig reaction with the ylide, derived from (5-phenoxypentyl)triphenylphosphonium bromide (**7a**) or (6-phenoxyhexyl)triphenylphosphonium bromide (**7b**) and KHMDS, afforded exclusively the Z olefins **14a−c** ($J_{H2'-H3'}$ = 11.1 Hz) in excellent yields (96−97%).[35,37] In turn, the required phosphonium salts **7a** or **7b** were synthesized from commercially available 5-phenoxypentylbromide (**6a**) or 6-phenoxyhexylbromide (**6b**), respectively, and triphenylphosphine in refluxing benzene.[37] Catalytic hydrogenation of the double bond in **14a−c** proceeded in excellent yields (98%) by

https://dx.doi.org/10.1021/acs.jmedchem.0c02053
J. Med. Chem. 2021, 64, 3870−3884

Scheme 2[a]

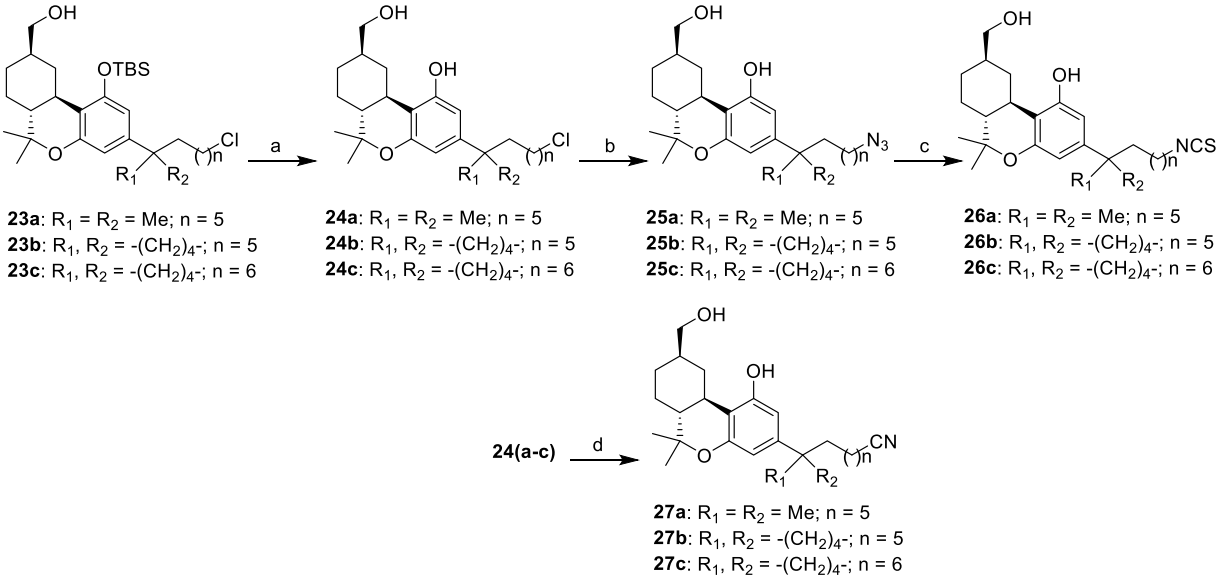

[a]Reagents and conditions: (a) *n*-Bu_4NF, THF, −78 °C, 10 min, 95−98%; (b) TMG-N_3, $CHCl_3/CH_3NO_2$, 70 °C, 30 h, 84−88%; (c) CS_2, PPh_3, THF, r t, 18 h, 76−87%; and (d) NaCN, DMSO, r t, 18 h, 77−85%.

Scheme 3[a]

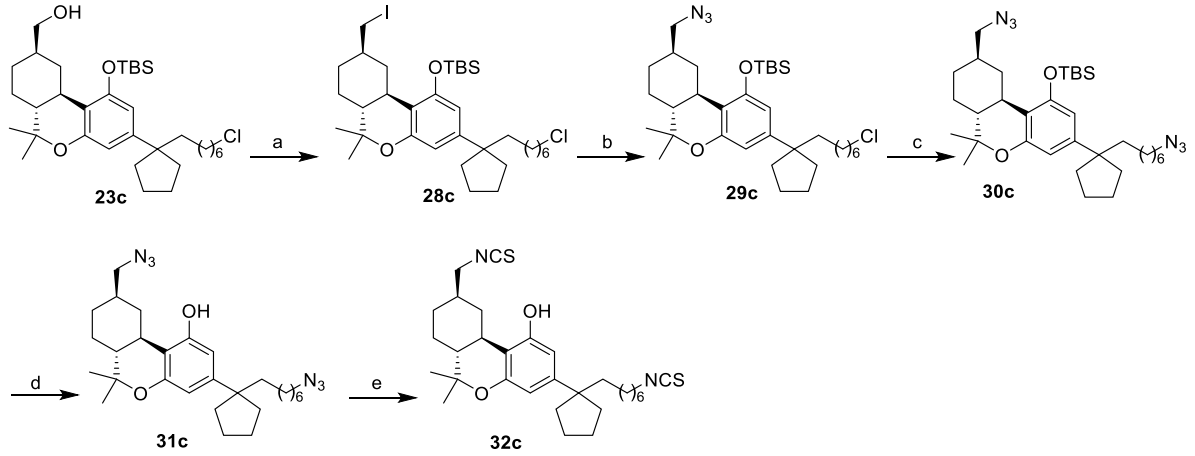

[a]Reagents and conditions: (a) I_2, imidazole, PPh_3, benzene, 50 °C, 30 min, 95%; (b) $(n\text{-}Bu)_4N^+N_3^-$, CH_2Cl_2, r t, 30 h, 83%; (c) TMG-N_3, $CHCl_3/CH_3NO_2$, 70 °C, 30 h, 74%; (d) *n*-Bu_4NF, THF, −78 °C, 30 min, 92%; and (e) CS_2, PPh_3, THF r t, 18 h, 86%.

using 10% Pd/C in ethyl acetate. This was followed by exposure of the intermediate alkanes **15a−c** to boron tribromide which cleaved the ether groups and introduced the C7′ and C8′ bromo group for resorcinols **16a−c** (91−92% yields).[37,39] Following our modifications of an original procedure, the mixture of the chiral terpene diacetates **10** was produced in two steps from commercially available (1*R*)-(+)-nopinone (**8**).[43,47,48] Condensation of **10** with resorcinols **16a−c** led to norpinanones **17a−c** (59−64% yields) which upon treatment with catalytic trimethylsilyl triflate gave the 9-keto-HHCs **18a−c** (70−75%) with the required (6a*R*, 10a*R*) stereochemistry.[37,48]

At this point, we envisioned that ω-substituted chlorides (*i.e.*, **23a−c**) could be very useful as common synthetic intermediates for the preparation of the monofunctionalized, as well as the bifunctionalized probes. This will significantly reduce the synthetic effort required for the multi-step synthesis of all analogues pursued in this study. Thus, exposure of **18a−c** to TBSCl, imidazole, and DMAP in the presence of dimethylformamide at 62 °C effectively protects the free phenolic hydroxyl group and displaces the bromine with chlorine in a single step producing the key synthetic intermediates **19a−c** in high yields (91−93%).[41,49] Treatment of commercially available (methoxymethyl)-triphenylphosphonium chloride with KHMDS and coupling of the *in situ* formed ylide with the 9-keto-cannabinoids **19a−c** gave the respective enol ethers **20a−c** (70−73% yields) as 2:1 mixtures of two isomers (see the Supporting Information) based on ^{1}H NMR analysis.[41,44] Subsequently, the methyl vinyl ethers **20a−c** were hydrolyzed with wet trichloroacetic acid (90−95% yields), and the resulting diastereomeric mixture of C9 aldehydes **21a−c** (2:1 ratio by ^{1}H NMR) was epimerized to give the β-equatorial isomers **22a−c** in 80−84% yields.[41,44] Finally, reduction with sodium borohydride afforded the key 11-hydroxy-chlorides **23a−c** in high yields (97−98%).

https://dx.doi.org/10.1021/acs.jmedchem.0c02053
J. Med. Chem. 2021, 64, 3870−3884

Scheme 4[a]

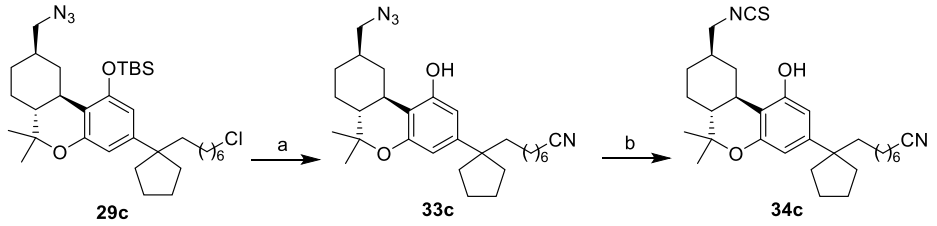

[a]Reagents and conditions: (a) NaCN, DMSO, r t, 15 h, 57% and (b) CS_2, PPh_3, THF, r t, 18 h, 78%.

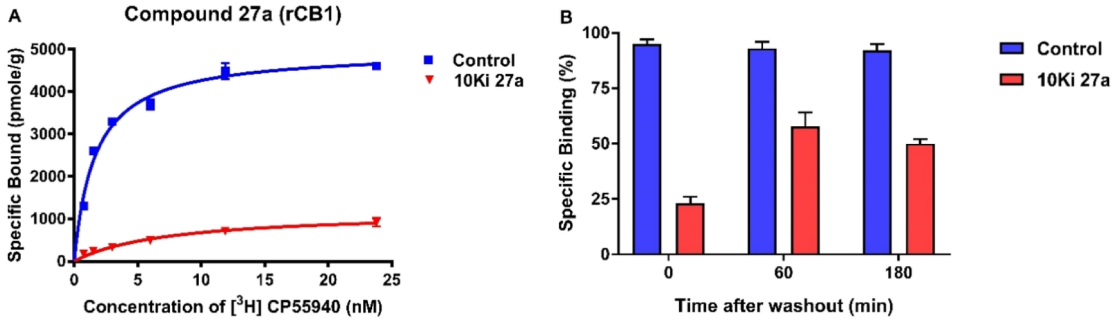

Figure 2. (A) Cell membranes were pretreated with **27a** (4 nM) or buffer (control) for 1 h, washed three times, and then subjected to [^{3}H]CP-55,940 binding. (B) B_{max} values (maximal binding capacity) were calculated from (A) where the incubation time was increased following the washing. Data represent the mean values ± SEM of at least three independent experiments performed in duplicate.

Synthesis of the side-chain monofunctionalized probes was accomplished, as shown in Scheme 2. Thus, 11-hydroxy-intermediates **23a−c** were treated with tetra-*n*-butylammonium fluoride (TBAF) to give the C7′/C8′-chloro-cannabinoids **24a−c** in high yields (95−98%).[41,44] Displacement of the chloride in HHC **24a−c** by *N*,*N*,*N*′,*N*′-tetramethylguanidinium azide led to monofunctionalized C7′/C8′ azide probes **25a−c** (84−88% yields).[25] Exposure of these analogues first to triphenylphosphine and then to carbon disulfide converted the azide to isothiocyanate, leading to the respective probes **26a−c** (76−87% yields).[25,50] Treatment of chlorides **24a−c** with sodium cyanide afforded the C7′ and C8′ cyano-probes **27a−c** in high yields (77−85%).[37]

The heterobifunctionalized cannabinoid ligands represent a much greater challenge to the synthetic chemist. This challenge is imposed by the need to introduce regioselectively two reactive groups within the molecule. We have found an efficient approach to accomplish this task which takes advantage of the different reactivities of the alkyl chlorides and iodides under conditions of nucleophilic substitution. Thus, the synthesis of both homo- and heterobifunctionalized probes proceeded in high overall yields from the common key intermediate 8′-chloro-11-iodo-HHC **28c** with complete control of the halogen substitution under the experimental conditions used. Synthesis of the homo-bifunctionalized azido and isothiocyanato probes carrying a cyclopentyl ring at the C1′ is depicted in Scheme 3. The 11-hydroxy-HHC chloride **23c** was converted to the requisite 8′-chloro-11-iodo-HHC analogue **28c** in 95% yield by using the triphenylphosphine, iodine, imidazole method.[39] The first azide displacement reaction occurs exclusively at C11 and in high yield (83%) upon exposure of **28c** to tetra-*n*-butylammonium azide at room temperature. The second azide displacement at C8′ was accomplished by treatment of the 8′-chloro-11-azido-HHC analogue **29c** with *N*,*N*,*N*′,*N*′-tetramethylguanidinium azide in chloroform/nitromethane at 70 °C to give **30c** (74% yield). This was followed by cleavage of the silyl ether at C1 using TBAF to produce the di-azido-probe **31c** in 92% yield. The subsequent Staudinger reactions worked well at both the C11 and the C8′ azido groups and afforded the homo-bifunctionalized isothiocyanato ligand **32c** in a single operation and in high yield (86%). The intermediate C11 azide **29c** served as the starting point for the synthesis of the hetero-bifunctionalized probes **33c** and **34c** (Scheme 4). Thus, treatment of chloride **29c** with sodium cyanide displaces the chlorine atom at the side chain and cleaves the phenyl silyl ether in one step, leading to compound **33c** (57% yield). The most reactive isothiocyanato group in the hetero-bifunctionalized probe **34c** was introduced in the last synthetic step by exposure of the azide **33c** to Staudinger conditions (78% yield).

Binding Affinities on CB1 and CB2 Receptors. The abilities of the ligands **25a−c**, **26a−c**, **27a−c**, **31c**, **32c**, **33c**, and **34c** to displace [^{3}H]CP-55,940 from membranes prepared from rat brain (source of CB1) and HEK 293 cells expressing either mouse or human CB2 were determined, as described earlier,[37,38] and inhibition constant values (K_i) from the respective competition binding curves are given in Table 1. The use of two CB2 receptor preparations was aimed at addressing species differences that we have observed earlier.[51] The compounds of this study are HHC analogues with one group at the ω-position (C7′/C8′) of the C3 side-chain (monofunctionalized probes) or two groups (bifunctionalized probes) at both the C8′ and the C11 of the HHC structure. The seven or eight carbon long side chains of the monofunctionalized ligands carry a *gem*-dimethyl or a cyclopentyl substituent at C1′ while the bifunctionalized ligands bear a cyclopentyloctyl chain at C3. In agreement with our rational design, the monofunctionalized ligands have remarkably high binding affinities for both CB1 and CB2 receptors with most of their K_i values being in the picomolar range and they do not exhibit species differences. The monofunctional-

https://dx.doi.org/10.1021/acs.jmedchem.0c02053
J. Med. Chem. 2021, 64, 3870−3884

Table 1. Affinities (K_i) and Reductions in the Specific Binding (B_{max}) of [^{3}H]CP-55,940 after Ligand Pretreatment of Mono- and Bifunctionalized Classical Cannabinoid Probes for the CB1 and CB2 CBRs

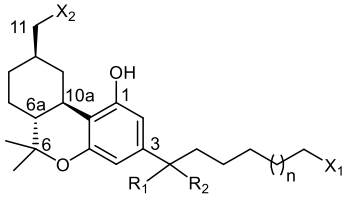

cmpd	X_1	X_2	n	R_1, R_2	(K_i, nM)[a]			B_{max} reduction (%)[b]	
					rCB1	mCB2	hCB2	CB1	CB2
2a	-H	-OH	2		3.0 ± 0.8	-	2.1 ± 0.6	NR[c]	NR[c]
25a	-N_3	-OH	2		0.41 ± 0.05	0.8 ± 0.1	1.40 ±0.06	75 ± 7	63 ± 4
25b	-N_3	-OH	2		0.4 ± 0.1	0.8 ± 0.1	0.8 ± 0.4	87 ± 8	65 ± 6
25c	-N_3	-OH	3		0.5 ± 0.2	1.6 ± 0.1	1.5 ± 0.3	48 ± 4	37 ± 2
26a	-NCS	-OH	2		0.39 ± 0.04	0.8 ± 0.1	3.15±0.04	65 ± 5	75 ± 5
26b	-NCS	-OH	2		1.1 ± 0.1	0.9 ± 0.2	1.3 ± 0.5	39 ± 3	34 ± 3
26c	-NCS	-OH	3		0.4 ± 0.1	1.1 ± 0.1	1.0 ± 0.2	51 ± 4	19 ± 2
27a	-CN	-OH	2		0.40 ± 0.05	0.8 ± 0.1	0.4 ± 0.1	76 ± 5	60 ± 4
27b	-CN	-OH	2		0.8 ± 0.2	1.0 ± 0.1	1.4 ± 0.2	68 ± 5	45 ± 3
27c	-CN	-OH	3		0.5 ± 0.1	0.9 ± 0.1	0.40 ±0.05	60 ± 4	40 ± 3
31c	-N_3	-N_3	3		0.7 ± 0.1	1.2 ±0.2	1.5 ± 0.2	28 ± 2	21 ± 1
32c	-NCS	-NCS	3		37.6 ± 0.6	14.6 ± 2.1	4.2 ± 0.3	37 ± 3	15 ± 1
33c	-CN	-N_3	3		0.3 ± 0.1	1.4 ± 0.2	0.3±0.1	NR[c]	NR[c]
34c	-CN	-NCS	3		0.4 ± 0.1	1.9 ± 0.3	0.6 ± 0.2	NR[c]	NR[c]

[a]Affinities for CB1 and CB2 were determined using rat brain membranes (CB1) or membranes from HEK293 cells expressing mouse or human CB2 and [^{3}H]CP-55,940 as the radioligand following previously described procedures. Data were analyzed using nonlinear regression analysis. K_i values were obtained from three independent experiments performed in triplicate and are expressed as the mean of the three values with ± SEM. [b]Data are presented as mean with ± SEM of at least three experiments performed in duplicate. The receptor membranes were pretreated with concentrations equal to 10-fold the compound's K_i value. Percentage was calculated as: $\{[B_{max}(\text{control}) - B_{max}(\text{ligand})]/B_{max}(\text{control})\}F \times 100$. B_{max}(ligand), as described under the Experimental Section. The B_{max}(control) for [^{3}H]-CP-55,940 was determined by conducting the assay as described but in the absence of the test ligand. [c]NR: no reduction.

https://dx.doi.org/10.1021/acs.jmedchem.0c02053
J. Med. Chem. 2021, 64, 3870−3884

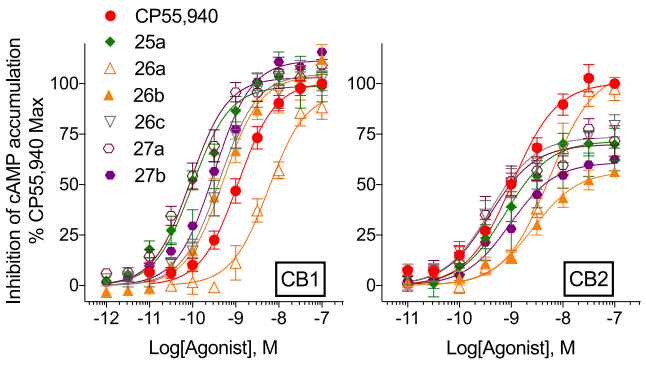

Figure 3. Concentration-dependent inhibition of forskolin-stimulated cAMP accumulation in cells expressing either hCB1 (left) or hCB2 (right) receptors by representative ligands. Data are the mean with SEM; CP-55,940 was assessed in parallel for all assays and data were normalized to 100 nM CP-55,930 maximum response (n = 12 for CB1 and 11 for CB2); all other agonists represent the mean ± SEM of 4−8 experiments performed in duplicate.

Table 2. Functional Data[a] of Selected Probes for the hCB1 and hCB2 Receptors in the Forskolin-Stimulated Adenylyl Cyclase Assay

CB1 cAMP	E_{max} % 100 nM CP	95% CI	nM EC_{50}	95% CI nM
CP-55,940	100		1.13	(0.87−1.46)
25a	99	(93−104)	0.098	(0.068−0.141)
26a	96	(86−107)	5.8	(3.8−8.7)
26b	104	(98−110)	0.52	(0.37−0.72)
26c	105	(98−111)	0.43	(0.30−0.60)
27a	103	(98−108)	0.088	(0.063−0.124)
27b	112	(105−118)	0.31	(0.22−0.44)
CB2 cAMP	E_{max} %100 nM CP	95% CI	nM EC_{50}	95% CI nM
CP-55,940	100		1.03	(0.74−1.43)
25a	72	(65−79)	0.77	(0.45−1.30)
26a	107	(96−118)	5.5	(3.6−8.2)
26b	57	(51−63)	2.7	(1.6−4.4)
26c	74	(68−80)	0.39	(0.24−0.62)
27a	70	(63−77)	0.38	(0.22−0.66)
27b	61	(53−70)	0.96	(0.45−1.95)

[a]Data presented as mean with 95% confidence intervals are shown: EC_{50}, half-maximum effective concentration; E_{max}, percentage of maximum response relative to 100 nM CP-55.940, curves are presented in Figure 3.

ized probes show significant increase in binding affinity up to 8-fold for CB1 and 5-fold for CB2, when compared to the nonfunctionalized analogue **2a**. This suggests that within this structural motif: (a) both seven and eight carbon long-chain analogues substituted at C1′ with the *gem*-dimethyl or with the bulkier cyclopentyl groups can fit well within the binding pocket of CB1 and CB2, and (b) the presence of select groups (*i.e.*, N_3, NCS, and CN) at the ω-position of the chain in most cases increases the binding affinity of the monofunctionalized ligands compared to their non-functionalized surrogate.

A cursory examination of the binding affinity data of the side-chain monofunctionalized ligands **25c** and **27c** with their bifunctionalized counterparts **31c**, and **33c**, **34c**, respectively, indicates that for ligands carrying azido and cyano ω-substituted side chains, the replacement of the C11 hydroxy group with the azido or isothiocyanate moiety maintains the high binding affinity of the bifunctionalized ligand for both the CB1 and CB2 receptors. However, comparisons of the data of **32c** with those of **26c** and **34c** suggest that simultaneous incorporation of the electrophilic isothiocyanate at C8′ and C11 results in a reduction of the binding affinity of the ligand for both CB1 and CB2 receptors.

Tight Binding on CB1 and CB2 Receptors. The most prominent feature of the tight binding probes which differentiates them from other high-affinity binding ligands is their ability to bind insurmountably in a wash-resistant manner in each of the two receptors.[8,9] The ability of the mono- and bifunctionalized probes carrying isothiocyanato, azido, and cyano moieties to bind insurmountably in a wash-resistant manner on each of the two receptors was determined by measuring reductions in the saturation curve profile produced for the standard radioligand [^{3}H]CP-55,940, when the preparation was pretreated with the ligand being tested, and comparing it to the untreated sample. Following earlier work from our laboratory,[27] the experiment was conducted by pretreating the sample with concentrations equal to 10-fold the compound's K_i value for the receptor in question, washing the preparation with buffer three times, and subsequently measuring the decrease of B_{max} (maximal binding capacity) obtained from a saturation curve using [^{3}H]CP-55,940. Testing results are summarized in Table 1, while saturation binding curves for all analogues are provided under the Supporting Information. We expect that the effectiveness for tight binding for each ligand is determined by its ability to accurately fit within the receptors' orthosteric-binding pocket and being further enhanced by additional interactions (*e.g.*, hydrogen bonding, electrostatic, $\pi-\pi$ interactions, *etc.*). Our data clearly show that all the side-chain monofunctionalized probes (**25a−c**, **26a−c**, and **27a−c**) reduce the B_{max} of [^{3}H]CP-55,940 for both CB1 and CB2 receptors after extensive washing when compared to control. The non-functionalized analogue **2a** exhibits no reductions in the levels

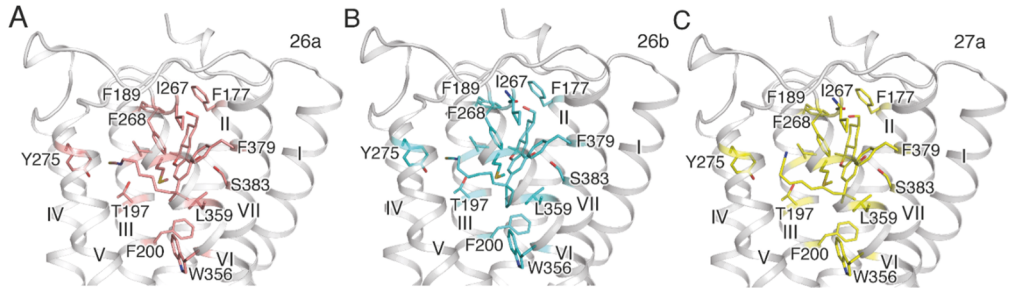

Figure 4. AM841 (**26a**) binding pocket analysis and molecular docking of **26b** and **27a** based on the hCB1 crystal structure (PDB: 5XR8). (A) Key residues involved in AM841 (pink sticks) binding. (B,C) Docking pose of **26b** (B, blue sticks) and **27a** (C, yellow sticks).

https://dx.doi.org/10.1021/acs.jmedchem.0c02053
J. Med. Chem. 2021, 64, 3870−3884

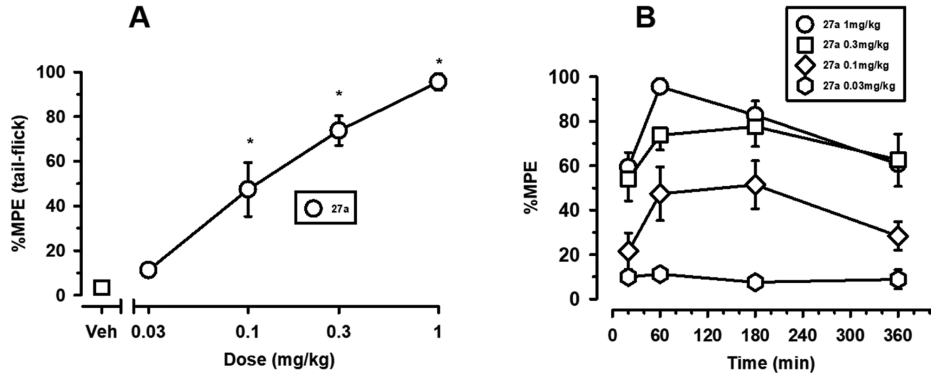

Figure 5. (A) Effects of **27a** (○), or vehicle (□) on antinociception using male CD-1 mice. Abscissa: dose in mg/kg. Ordinate: percentage of the maximum possible antinociceptive effect. Symbols represent the group mean ± SEM (n = 6/group). Asterisks indicate antinociceptive effects that are significantly different from vehicle, *p < 0.001. (B) Tail-flick latencies in a hot water bath (52 °C) after administration of four doses of **27a** at four time points (20, 60, 180, and 360 min post-administration) using male CD-1 mice (n = 6/dose). Abscissa: time (min) after injection. Ordinate: tail-flick withdrawal latencies expressed as a percentage of the maximum possible effect (% MPE; group mean ± SEM). For clarity in data presentation, data of vehicle group is not shown. The average antinociceptive effect of vehicle did not exceed 20% MPE at any of the four time points examined.

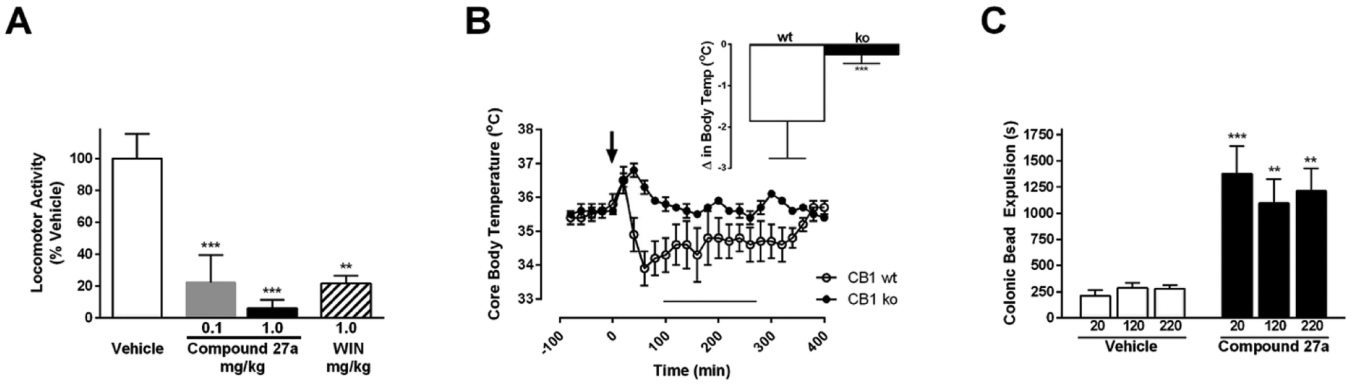

Figure 6. Effects of **27a** on spontaneous locomotion (A), thermoregulation (B), and colonic bead expulsion (C). Compound **27a** (0.1−1 mg/kg) dose-dependently reduced locomotion (A) and reduced core body temperature (B) in a CB1 receptor-specific manner and slowed colonic motility (C) at a dose of 0.1 mg/kg. Inset in (B) shows the maximum change in body temperature from mean baseline (−100 min before injection) over the time monitored post-injection (400 min). Note the very long-lasting effects of **27a** in both thermoregulation and bead expulsion. wt, wild-type mice; ko, CB1 receptor knockout mice. **P < 0.01, ***P < 0.001.

of B_{max} of [^{3}H]CP-55,940. Within the azido- and the cyano-substituted ligands, the highest reduction can be seen with those carrying the seven carbon long side chains. The C1′-*gem*-dimethyl-substituted isothiocyanato (NCS, **26a**) and cyano (CN, **27a**) probes exhibit the highest reduction for both CB1 and CB2, while the C1′-cyclopentyl-substituted azido (N_3, **25b**) ligand seems to be the best probe for photoirradiation experiments.[27,29] Moreover, a cursory examination of the data in Table 1 reveals that, in general, the synthesized probes exhibit slightly reduced results for the CB2 receptor when compared to CB1. The preference of the CB2 receptor for optimal side chains parallel those of CB1 for the azido (N_3, **25b**), isothiocyanato (NCS, **26a**), and cyano (CN, **27a**) probes.

In contrast to the electrophilic isothiocyanato group that can interact with cysteines[20] and the azido moiety that can interact with aminoacid residues after UV irradiation,[29] the aliphatic cyano group has not been shown to interact covalently with aminoacid residues. For this reason, in order to explore the time-dependent binding characteristics of the cyano-bearing cannabinergic probes, we sought to determine whether they can retain their tight binding properties over time. We selected probe **27a** as it showed the optimal results in the tight binding assay among the cyano probes **27a**−**c**. We followed a protocol, as described in our previous work,[8] where we pretreat CB1 membrane preparations with a concentration equal to 10-fold the K_i value of **27a**, then washed the preparation with buffer and subsequently measured the decrease of B_{max} obtained from a saturation curve using [^{3}H]CP-55,940 in different time points (60 and 180 min after the washout step). Based on the data summarized in Figure 2, cyano probe **27a** retains its tight binding profile by reducing the B_{max} of [^{3}H]CP-55,940 for at least 180 min after the washout step.

Comparisons of the side-chain cyclopentyloctyl di-azido **31c** and di-isothiocyanato **32c** ligands with their monofunctionalized counterparts **25c** and **26c**, respectively, shows a reduction in the tight binding properties of these homo-bifunctionalized probes. Within the cyclopentyloctyl side-chain structural motif, the hetero-bifunctionalized probes **33c** and **34c** exhibited no ability to reduce the specific binding of the radioligand. This indicates that the stereoelectronic requirements are more stringent for the bifunctionalized probes when compared to their monofunctionalized counterparts. This may be due to the presence of an 11-OH group in the monofunctionalized probes, as observed in the molecular docking process.

https://dx.doi.org/10.1021/acs.jmedchem.0c02053
J. Med. Chem. 2021, 64, 3870−3884

Functional Characterization. The long-term goal of this project was to develop mono- and bifunctionalized classical cannabinoid probes exhibiting tight binding characteristics and distinct agonist profiles. Thus, the monofunctionalized probes **25a**, **26b**, **26c**, **27a**, and **27b** were selected for further evaluation in assays assessing the regulation of adenylyl cyclase using overexpression systems of hCB1 and human CB2 (hCB2) receptors, as described in the Experimental Section.[8,9,11,52] In an earlier work, we have already reported that **26a** (AM841) behaves as a potent agonist at both the CB1 and CB2 receptors, which we designated as "megagonist."[8,19,20,30,32] In this study, we are focused on the above key analogues not only because they possess high CB1/CB2 receptor binding affinities and abilities to bind tightly in CB1 and/or CB2 binding sites but also because these ligands are representatives of all side-chain structural motifs that we explored in our study. The dose−response curves of the analogues for both the CB1 and CB2 are depicted in Figure 3 where data for the standard cannabinoid agonist CP-55,940 are also shown for comparison. Functional potencies (EC_{50}) and efficacies (E_{max}) of the ligands are presented in Table 2. Our testing results indicate that in the cyclase assay, all representative probes behave as highly potent and full efficacy agonists at the CB1 receptor as they all decrease the levels of forskolin-stimulated cAMP to the same extent as CP-55,940. Notably, among the compounds tested, the C7′-cyano-substituted analogue **27a** has distinguished itself as the most potent CB1 agonist with a potency (EC_{50} = 88 pM for CB1) much higher than that of the standard CB1/CB2 agonist CP-55,940. The exceedingly high potency of this compound leaves us to designate it as a "megagonist." Arguably, this property may be related to its ability to form a very tight complex with the CB1 receptor.

Molecular Docking. Based on the AM841 (**26a**)-bound hCB1 crystal structure (PDB: 5XR8),[8] we studied the interactions of representative side-chain agonists with the CB1 receptor through molecular docking (Figure 4A−C). We observe that all agonists adopt an L-shape conformation in the orthosteric-binding pocket. The interactions between the ligands and CB1 are mainly hydrophobic and aromatic. The tricyclic HHC ring system of all ligands forms $\pi-\pi$ interactions with $Phe268^{ECL2}$, $Phe379^{7.35}$, $Phe189^{3.25}$, and $Phe177^{2.64}$ (superscripts denote Ballesteros−Weinstein numbering),[53] while the phenolic hydroxyl at C1 of all analogues forms a hydrogen bond with $Ser383^{7.39}$. The hydroxy group at the C11 position of the ligands forms an additional hydrogen bond with the backbone carbonyl oxygen atom of $Ile267^{ECL2}$. The C3 alkyl chain of the three analogues extends into a long channel as we have reported earlier.[8] We also observe that the C3 alkyl chain of the most potent compound **27a** is in all-anti conformation with the lowest energy, while **26a** and **26b** are in mixed anti and gauche conformation.

***In Vivo* Behavioral Characterization.** In an earlier work, we have shown that the C1′-dimethyl-C7′-isothiocyanato-substituted analogue **26a** (AM841) behaved as an irreversible and remarkably potent cannabinergic agonist *in vitro*.[20,30,31] The ligand powerfully reduced gastrointestinal motility by acting on CB1 receptors in the small and large intestine under physiological conditions. However, AM841 did not exhibit characteristic centrally CB1 receptor-mediated effects (analgesia, hypothermia, or hypolocomotion) and behaved as a peripherally restricted ligand, showing very little brain penetration.[19] We have now explored key centrally and peripherally mediated *in vivo* effects of our newly identified C1′-dimethyl-C7′-cyano counterpart, **27a**, which also behaves as an exceptionally potent CB1 agonist *in vitro* (cAMP assay). Thus, cyano probe **27a** was studied in the centrally mediated CB1 receptor-characteristic nociception (Figure 5A,B) and locomotion and thermoregulation (Figure 6A,B, respectively) tests in mice. We also examined the magnitude and the duration of the effects of **27a** in the periphery using the colonic bead expulsion test (Figure 6C) to compare its effects with the peripherally restricted "megagonist" AM841.

The tail-flick latency procedure was used to measure the analgesic effects of **27a**. Animals were observed over a period of 6 h following drug or vehicle administration. The baseline latency for all the treatment conditions was 1.57 ± 0.5 s. Compound **27a** produced dose-dependent antinociceptive effects (Figure 5A), with 1 mg/kg producing maximal effects. Doses of 0.1−1 mg/kg **27a** had significant antinociceptive effects, as compared to vehicle ($p < 0.001$), with mean (±95% CI) ED_{50} value of 0.12 mg/kg (0.0859−0.1676). As shown in Figure 5B, **27a** has a fast onset of action and its antinociceptive effects lasted over 6 h. Two-way repeated measures ANOVA showed significant effects for dose (D) [$F_{(4,99)} = 40.441$; $p < 0.001$] and time (T) [$F_{(3,99)} = 7.102$; $p = 0.005$], with no significant interaction between $D \times T$. Compound **27a** had a quick onset of action (Figure 5B), at 20 min post-injection with 0.3 and 1 mg/kg producing significant antinociceptive effect, as compared to vehicle ($p < 0.001$). At 60 min post-injection, all the doses except 0.03 mg/kg produced peak antinociceptive effects, as compared to vehicle $p < 0.001$.

We then assessed the cyano probe **27a** for its effects in two additional assays of the cannabinoid tetrad,[54] hypolocomotion, and thermoregulation (Figure 6A,B, respectively). Here, we demonstrate that **27a** was highly potent as it reduced locomotion significantly (Figure 6A) and behaved as a CB1 receptor specific ligand in reducing body temperature (Figure 6B). Conversely, we had shown that compound **26a** was unable to produce neither hypolocomotion nor hypothermia.[19] Having established that the cyano probe **27a** shows centrally mediated CB1 effects, unlike its isothiocyanate congener **26a**, we compared the two ligands for their peripheral effects in reducing gastrointestinal motility. **27a** slowed colonic expulsion of a bead (Figure 6C) to the same extent as we have previously reported for **26a**.[19] Of note, the effect of the cyano probe **27a** barely waned after 4 h, whereas the isothiocyanate probe **26a**'s action was short lived.[19]

An overall comparison of the *in vivo* effects of the C1′-dimethyl-C7′-isothiocyanato analogue **26a** with the C1′-dimethyl-C7′-cyano counterpart **27a** indicates that although both compounds exhibit exceptionally high potency in the peripheral assay of colonic bead expulsion, only the cyano analogue **27a** induces potent centrally mediated cannabinergic effects. These data suggest that **27a** behaves as a globally (centrally and peripherally) acting CB1 "megagonist," while **26a** behaves as a peripherally restricted CB1 "megagonist."[19]

CONCLUSIONS

We report the development of novel cannabinergic ligands with remarkably high affinities for the CB1 and CB2 CBRs, which are powerful CB1/CB2 agonists with tight binding profiles. Our ligand design is based on the incorporation of select chemical groups at carefully chosen sites within the classical cannabinoid structure. These groups include the electrophilic isothiocyanato and the photoactivatable aliphatic

https://dx.doi.org/10.1021/acs.jmedchem.0c02053
J. Med. Chem. 2021, 64, 3870−3884

azido moieties, as well as the polar cyano. Our experiments indicate that all groups when introduced in the HHC template lead to tight binding interactions with the CBRs. Further evaluation of the wash-resistant binding profile of the C1′-dimethyl-C7′-cyano-substituted analogue **27a**, namely AM11245, showed that it can retain its tight binding profile. Representative probes behave as potent CB1 and CB2 agonists in the inhibition of the adenylyl cyclase assay. A striking finding is the exceptionally high potency of analogue **27a** (EC_{50} = 88 pM for CB1), as reflected by the cAMP assay, which we designated as "megagonist," a property that may be related to the tight binding interactions with the receptor.

The C1′-dimethyl-C7′-cyano- and C1′-dimethyl-C7′-isothiocyanato-substituted analogues **27a** (AM11245) and **26a** (AM841), respectively, were found to exhibit exceptionally high *in vivo* potency. Our studies indicate that **27a** is a globally acting CBR "megagonist" while **26a** is a "megagonist" restricted to the periphery.

EXPERIMENTAL SECTION

Materials. All reagents and solvents were purchased from Sigma-Aldrich Chemical Company, unless otherwise specified, and used without further purification. All anhydrous reactions were performed under a static argon atmosphere in the flame-dried glassware using scrupulously dry solvents. Flash column chromatography employed silica gel 60 (230−400 mesh). All compounds were demonstrated to be homogeneous by analytical TLC on pre-coated silica gel TLC plates (Merck, 60 F_{245} on glass, layer thickness 250 μm), and chromatograms were visualized by phosphomolybdic acid staining. Melting points were determined on a micro-melting point apparatus and are uncorrected. IR spectra were recorded on a PerkinElmer Spectrum One FT-IR spectrometer. Peak strength is indicated as w (weak) and s (strong). NMR spectra were recorded on a Bruker Ultra Shield 400 WB plus (^{1}H at 400 MHz, ^{13}C at 101 MHz) or on a Varian INOVA-500 (^{1}H at 500 MHz, ^{13}C at 126 MHz) spectrometer, and chemical shifts are reported in units of δ relative to internal TMS. Multiplicities are indicated as br (broadened), s (singlet), d (doublet), t (triplet), q (quartet), and m (multiplet), and coupling constants (J) are reported in hertz (Hz). Low- and high-resolution mass spectra were performed in the School of Chemical Sciences, University of Illinois at Urbana-Champaign. Mass spectral data are reported in the form of m/z (intensity relative to base = 100). Purities of compounds were determined by HPLC/MS analysis using a Waters MicroMass ZQ system [electrospray-ionization (ESI)] with Waters-2525 binary gradient module coupled to a Photodiode Array Detector (Waters-2996) and ELS detector (Waters-2424) using a XTerra MS C18, 5 μm, 4.6 mm × 50 mm column and acetonitrile/water; all tested compounds were >95% pure.

*{[(6aR,9R,10aR)-3-[1-(7-Chloroheptyl)cyclopentyl)]-9-(iodomethyl)-6,6-dimethyl-6a,7,8,9,10,10a-hexahydro-6H-benzo[c]chromen-1-yl]oxy}(tert-butyl)dimethylsilane (**28c**).* To a solution of **23c** (461 mg, 0.8 mmol) in anhydrous benzene (16 mL), under an argon atmosphere, were added imidazole (217 mg, 3.2 mmol) and triphenylphosphine (419.7 mg, 1.6 mmol), then the reaction mixture was heated to 50 °C, followed by a dropwise addition of a solution of iodine (406 mg, 1.6 mmol) in benzene. The reaction mixture was stirred for 30 min at 50 °C. The reaction was quenched by an aqueous sodium sulfite solution. Extractive isolation with diethyl ether and purification by flash column chromatography on silica gel (0−15% diethyl ether in hexane) gave **28c** (521 mg, 95% yield) as a white viscous oil. IR (neat) 2929, 2857, 1612, 1562, 1411, 1361, 1324, 1253, 1058, 835, 779 cm^{-1}; ^{1}H NMR (500 MHz, $CDCl_3$): δ 6.33 (d, J = 1.9 Hz, 1H, Ar-H), 6.26 (d, J = 1.9 Hz, 1H, Ar-H), 3.48(t, J = 6.9 Hz, 8′-H) 3.26−3.19 (dd and m as d overlapping, 2H, 1H of C-ring, 1H of $-CH_2I$, especially, m as br d, J = 12.8 Hz, 1H, C-ring, 3.21, dd, J = 9.7,4.8 Hz, half of an AB system, 1H, $-CH_2I$) 3.08 (dd, J = 9.7, 7.1 Hz, half of an AB system, 1H, $-CH_2I$), 2.40−2.33 (m as td, J = 11.0, 2.6 Hz, 1H, C-ring), 2.12−2.05 (m, 1H, C-ring), 1.92−1.88 (m, 1H, C-ring), 1.87−1.78 (m, 2H, the cyclopentyl ring), 1.76−1.58 (m, 9H, 6H of the cyclopentyl ring, 2H of the side chain, 1H of C-ring), 1.52−1.44 (m, 3H, 2′-H, C-ring), 1.38 (s, 3H, 6-Me), 1.36−1.29 (m, 2H, side chain), 1.22−1.10 (m, 6H, 4H of the side chain, 2H of C-ring), 1.05 (s, 3H, 6-Me), 1.02−0.93 (s and m overlapping, 11H, 2H of the side chain, $Si(Me)_2CMe_3$, especially, 1.00, s, 9H, $Si(Me)_2CMe_3$), 0.89−0.82 (m, 1H, C-ring), 0.22 (s, 3H, $Si(Me)_2CMe_3$), 0.13 (s, 3H, $Si(Me)_2CMe_3$). ^{13}C NMR (100 MHz $CDCl_3$): δ 154.3, 154.1, 148.5, 113.0, 110.8, 109.4, 50.6, 49.2, 45.1, 41.8, 49.7, 37.6, 37.0, 35.5, 33.5, 32.6, 30.1, 29.9, 28.7, 27.6, 27.5, 26.8, 26.0, 25.2, 23.3, 18.7, 18.3, 15.1 ($-CH_2I$), −3.8, −4.6. Mass spectrum (ESI) m/z (relative intensity): 687 (M^+ + H, 100). HPLC analysis showed a retention time of 8.0 min for the title compound.

*{[(6aR,9R,10aR)-9-(Azidomethyl)-3-[1-(7-chloroheptyl)-cyclopentyl]-6,6-dimethyl-6a,7,8,9,10,10a-hexahydro-6H-benzo[c]-chromen-1-yl]oxy}(tert-butyl)dimethylsilane (**29c**).* To a solution of **28c** (528 mg, 0.77 mmol) in anhydrous CH_2Cl_2 (15.5 mL) at r t, under an argon atmosphere, was added tetrabutylammonium azide (1.6 g, 7.7 mmol). The reaction mixture was stirred for 30 h at the same temperature and then quenched by brine. Extractive isolation with diethyl ether and purification by flash column chromatography on silica gel (0−10% diethyl ether in hexane) gave **29c** (384 mg, 83% yield) as a white foam. IR (neat): 2929, 2858, 2097 (s, N_3), 1612, 1563, 1463, 1411, 1342, 1254 1138, 1062, 873 cm^{-1}; ^{1}H NMR (500 MHz, $CDCl_3$): δ 6.33 (d, J = 1.9 Hz, 1H, Ar-H), 6.26 (d, J = 1.9 Hz, 1H, Ar-H), 3.48 (t, J = 6.9 Hz, 8′-H) 3.23−3.17 (dd and m as d overlapping, 2H, 1H of C-ring, 1H of $-CH_2N_3$, especially, m, 1H, C-ring, 3.21, dd, J = 12.1, 6.1 Hz, half of an AB system, 1H, $-CH_2N_3$) 3.14 (dd, J = 12.1, 7.1 Hz, half of an AB system, 1H, $-CH_2N_3$), 2.38−2.31 (m as td, J = 11.1, 2.7 Hz, 1H, C-ring), 2.02−1.97 (m, 1H, C-ring), 1.92−1.88 (m, 1H, C-ring), 1.87−1.73 (m, 3H, 2H of the cyclopentyl ring, 1H of C-ring), 1.76−1.58 (m, 8H, 6H of the cyclopentyl ring, 2H, side chain), 1.52−1.44 (m, 3H, 2′-H, C-ring), 1.38 (s, 3H, 6-Me), 1.35−1.28 (m, 2H, side chain), 1.24−1.10 (m, 6H, 4H of the side chain, 2H of C-ring), 1.05 (s, 3H, 6-Me), 1.02−0.91 (s and m overlapping, 11H, 2H of the side chain, $Si(Me)_2CMe_3$, especially, 1.00, s, 9H, $Si(Me)_2CMe_3$), 0.86−0.79 (m, 1H, C-ring), 0.22 (s, 3H, $Si(Me)_2CMe_3$), 0.13 (s, 3H, $Si(Me)_2CMe_3$). ^{13}C NMR (100 MHz $CDCl_3$): δ 154.4, 154.2, 149.3, 113.5, 110.8, 109.5, 57.8, 51.5, 50.4, 49.1, 41.6, 40.5, 37.7, 37.5, 34.9, 34.1, 30.6, 29.9, 28.8, 28.7, 27.6, 27.3, 26.6, 25.9, 25.0, 23.2, 18.6, 18.1, −3.6, −4.3. Mass spectrum (ESI) m/z (relative intensity): 602 (M^+ + H, 100). HPLC analysis showed a retention time of 9.1 min for the title compound.

*{[(6aR,9R,10aR)-3-[1-(7-Azidoheptyl)cyclopentyl]-9-(azidomethyl)-6,6-dimethyl-6a,7,8,9,10,10a-hexahydro-6H-benzo[c]chromen-1-yl]oxy}(tert-butyl)dimethylsilane (**30c**).* To a solution of **29c** (186 mg, 0.31 mmol) in anhydrous CH_2Cl_2 (5.2 mL) at r t, under an argon atmosphere, was added *N*,*N*,*N*′,*N*′-tetramethylguanidinium azide (1.4 g, 9.1 mmol), and the reaction mixture was heated at 70 °C for 30 h. On completion, the reaction was quenched with water and diluted with CH_2Cl_2. The organic phase was washed with brine, dried over $MgSO_4$, and concentrated in vacuo. Purification by flash column chromatography on silica gel (3−8% diethyl ether in hexanes) gave 151 mg of **30c** as a white foam in 74% yield. IR (neat): 2928, 2857, 2097 (s, N_3), 1756, 1612, 1411, 1342, 1254, 1138, 1062, 839 cm^{-1}; ^{1}H NMR (500 MHz, $CDCl_3$): δ 6.33 (d, J = 1.9 Hz, 1H, Ar-H), 6.26 (d, J = 1.9 Hz, 1H, Ar-H), 3.24−3.15 (dd, t and m as d overlapping, 3H, C-ring, $-CH_2N_3$, 8′-H, especially, 3.21, t, J = 6.9 Hz, 8′-H, m as br d, J = 12.8 Hz, 1H, C-ring, 3.21, dd, J = 121, 6.1 Hz, half of an AB system, 1H, $-CH_2N_3$) 3.14 (dd, J = 12.1, 7.1 Hz, half of an AB system, 1H, $-CH_2N_3$), 2.38−2.31 (m as td, J = 11.1, 2.7 Hz, 1H, C-ring), 2.02−1.97 (m, 1H, C-ring), 1.92−1.88 (m, 1H, C-ring), 1.87−1.73 (m, 3H, 2H of the cyclopentyl ring, 1H of C-ring), 1.71−1.58 (m, 6H, cyclopentyl ring), 1.54−1.43 (m, 5H, 4H of the side-chain group, 1H of C-ring), 1.38 (s, 3H, 6-Me), 1.31−1.24 (m, 2H, side chain), 1.21−1.10 (m, 6H, 4H of the side chain, 2H of C-ring), 1.06 (s, 3H, 6-Me), 1.02−0.91 (s and m overlapping, 11H, 2H of the side chain, $Si(Me)_2CMe_3$, especially, 1.00, s, 9H, $Si(Me)_2CMe_3$), 0.84−0.76 (m, 1H, C-ring), 0.24 (s, 3H, $Si(Me)_2CMe_3$), 0.12 (s, 3H, $Si(Me)_2CMe_3$). ^{13}C NMR (100 MHz $CDCl_3$): δ 154.3, 154.1, 149.1,

https://dx.doi.org/10.1021/acs.jmedchem.0c02053
J. Med. Chem. 2021, 64, 3870−3884

113.6, 110.8, 109.5, 57.8, 51.5, 50.5, 49.0, 41.6, 38.2, 37.7, 37.5, 34.9, 34.1, 30.6, 29.8, 28.9, 28.7, 27.7, 27.4, 26.6, 25.9, 25.0, 23.2, 18.6, 18.1, −3.6, −4.3. Mass spectrum (ESI) m/z (relative intensity): 609 (M^+ + H, 100). HPLC analysis showed a retention time of 8.8 min for the title compound.

*(6aR,9R,10aR)-3-[1-(7-Azidoheptyl)cyclopentyl]-9-(azidomethyl)-6,6-dimethyl-6a,7,8,9,10,10a-hexahydro-6H-benzo[c]chromen-1-ol (**31c**).* To a solution of **30c** (150 mg, 0.24 mmol) in anhydrous THF (6.1 mL) at −78 °C, under an argon atmosphere, was added TBAF (0.3 mL, 0.3 mmol, 1 M solution in anhydrous THF). The reaction mixture was stirred for 30 min at the same temperature and then quenched using a saturated aqueous ammonium chloride solution. Extractive isolation with diethyl ether and purification by flash column chromatography on silica gel (8−25% ethyl acetate in hexane) gave **31c** (114 mg, 92% yield) as a white foam. IR (neat): 2931, 2861, 2097 (s, N_3), 1756, 1622, 1413, 1331, 1251, 1138, 1039, 839 cm^{-1}; ^1H NMR (500 MHz, $CDCl_3$): δ 6.29 (d, J = 1.9 Hz, 1H, Ar-H), 6.14 (d, J = 1.9 Hz, 1H, Ar-H), 5.12 (br s, 1H, OH) 3.27−3.19 (dd, t and m as d overlapping, 3H, C-ring, $-CH_2N_3$, 8′-H, especially, 3.21, t, J = 6.9 Hz, 8′-H, m as br d, J = 12.8 Hz, 1H, C-ring, 3.21, dd, J = 12.1, 6.1 Hz, half of an AB system, 1H, $-CH_2N_3$) 3.15 (dd, J = 12.1, 7.1 Hz, half of an AB system, 1H, $-CH_2N_3$), 2.51−2.43 (m as td, J = 11.1, 2.7 Hz, 1H, C-ring), 2.02−1.97 (m, 1H, C-ring), 1.95−1.88 (m, 1H, C-ring), 1.87−1.75 (m, 3H, 2H of the cyclopentyl ring, 1H of C-ring), 1.73−1.58 (m, 6H, cyclopentyl ring), 1.55−1.42 (m, 5H, 4H of $-CH_2-$ of the side-chain group, 1H of C-ring), 1.38 (s, 3H, 6-Me), 1.31−1.24 (m, 2H, the side chain), 1.21−1.10 (m, 6H, 4H of the side chain, 2H of C-ring), 1.08 (s, 3H, 6-Me), 1.04−0.93 (m, 2H side chain), 0.85−0.81 (m as q, J = 11.9 Hz, 1H, C-ring). ^{13}C NMR (100 MHz $CDCl_3$): δ 154.4, 154.1, 149.1, 109.2, 108.8, 106.3, 57.8, 51.4, 50.6, 49.1, 41.7, 38.1, 37.5, 37.4, 35.0, 34.2, 30.8, 30.0, 28.9, 28.7, 27.7, 27.3, 26.6, 25.0, 23.3, 19.0. Mass spectrum (ESI) m/z (relative intensity): 495 (M^+ + H, 100). Exact mass (ESI) calculated for $C_{28}H_{43}N_6O_2$ (M^+ + H), 495.3447; found 495.3440. HPLC analysis showed a retention time of 6.1 min for the title compound.

*(6aR,9R,10aR)-3-[1-(7-Isothiocyanatoheptyl)cyclopentyl]-9-(isothiocyanatomethyl)-6,6-dimethyl-6a,7,8,9,10,10a-hexahydro-6H-benzo[c]chromen-1-ol (**32c**).* To a solution of **31c** (65 mg, 0.13 mmol), in anhydrous THF (4.3 mL) at room temperature, was added triphenyl phosphine (340 mg, 1.3 mmol). Anhydrous carbon disulfide (0.48 mL, 8.0 mmol) was then added dropwise, and the reaction mixture was stirred for an additional 18 h at the same temperature. Upon completion, the reaction mixture was concentrated under reduced pressure and purified by flash column chromatography on silica gel (50−80% diethyl ether in hexanes) to give 59 mg of **32c** in 86% yield as light-yellow foam. IR (neat): 2923, 2859, 2106 (s, NCS), 1728, 1618, 1574, 1413, 1372, 1339, 1251, 1139, 1036, 863 cm^{-1}; ^1H NMR (500 MHz, $CDCl_3$): δ 6.30 (d, J = 1.9 Hz, 1H, Ar-H), 6.14 (d, J = 1.9 Hz, 1H, Ar-H), 4.90 (br s, 1H, OH) 3.51−3.44 (dd and t, 2H, $-CH_2NCS$, 8′-H, especially, 3.49, t, J = 6.9 Hz, 8′-H, m as br d, J = 12.6 Hz, 1H, C-ring, 3.21, dd, J = 14.2, 5.5 Hz, half of an AB system, 1H, $-CH_2NCS$), 3.41 (dd, J = 14.2, 6.4 Hz, half of an AB system, 1H, $-CH_2NCS$), 3.29−3.23(m as br d, J = 12.6 Hz, 1H, C-ring), 2.53−2.45 (m as td, J = 11.2, 2.7 Hz, 1H, C-ring), 2.02−1.90 (m, 2H, C-ring), 1.86−1.78 (m, 2H, the cyclopentyl ring), 1.73−1.58 (m, 9H, 6H of cyclopentyl ring, 1H of C-ring, 2H of the side chain), 1.53−1.44 (m, 3H, 2H of the side chain, 1H of C-ring), 1.39 (s, 3H, 6-Me), 1.34−1.26 (m, 2H, of the side chain), 1.23−1.11 (m, 6H, 4H of the side chain, 2H of C-ring), 1.09 (s, 3H, 6-Me), 1.04−0.93 (m, 2H, side chain), 0.92−0.89 (m as q, J = 11.9 Hz, 1H, C-ring). ^{13}C NMR (100 MHz $CDCl_3$): δ 154.4, 154.1, 149.2, 130.1 (NCS), 108.9, 108.7, 106.4, 50.9, 50.6, 48.8, 45.0, 41.6, 38.5, 37.5, 37.4, 34.9, 33.8, 30.4, 29.9, 29.8, 28.5, 27.7, 27.2, 26.4, 24.9, 23.3, 19.0. Mass spectrum (ESI) m/z (relative intensity): 527 (M^+ + H, 100). Exact mass (ESI): calcd for $C_{30}H_{43}N_2O_2S_2$ (M^+ + H), 527.2766; found, 527.2776. HPLC analysis showed a retention time of 6.4 min for the title compound.

*8-(1-((6aR,9R,10aR)-9-(Azidomethyl)-1-hydroxy-6,6-dimethyl-6a,7,8,9,10,10a-hexahydro-6H-benzo[c]chromen-3-yl)cyclopentyl)-octanenitrile (**33c**).* To a solution of **29c** (120 mg, 0.2 mmol) in anhydrous DMSO (4 mL) at room temperature, was added sodium azide (100 mg, 2.1 mmol). The reaction mixture was stirred for an additional 15 h at the same temperature. The reaction mixture was quenched by the addition of ice-cold water and diluted with diethyl ether and was stirred for 30 min. The two phases were separated, and the aqueous layer was extracted with diethyl ether. The combined organic layer was washed with brine, dried over $MgSO_4$, and evaporated under reduced pressure. Purification by flash column chromatography on silica gel (20−60% diethyl ether in hexane) gave **33c** (55 mg, 57% yield) as light-yellow foam. IR (neat): 3394 (OH), 2929, 2859, 2252 (w, CN), 2096 (s, N_3), 1621, 1573, 1455, 1414, 1137, 1037, 838 cm^{-1}; ^1H NMR (500 MHz, $CDCl_3$): δ 6.29 (d, J = 1.8 Hz, 1H, Ar-H), 6.15 (d, J = 1.8 Hz, 1H, Ar-H), 4.87 (br s, 1H, Ar-OH), 3.28−3.13 (m and dd overlapping, 3H, 1H of C-ring, 2H of $-CH_2N_3$, especially, m as br d, J = 12.4 Hz, 1H, C-ring, 3.21, dd, J = 12.0, 6.0 Hz, half of an AB system, 1H, ($-CH_2N_3$) 3.14, dd, J = 12.0, 7.0 Hz, half of an AB system, 1H, ($-CH_2N_3$), 2.47 (m as td, J = 11.2 Hz, J = 2.7 Hz, 1H, C-ring), 2.31 (t, J = 7.1 Hz, 2H, H-8′), 2.02−1.97 (m, 1H, C-ring), 1.95−1.88 (m, 1H, C-ring), 1.87−1.75 (m, 3H, 2H of the cyclopentyl ring, 1H of C-ring), 1.73−1.58 (m, 6H, cyclopentyl ring), 1.55−1.42 (m, 5H, 4H of the side chain, 1H of C-ring), 1.38 (s, 3H, 6-Me), 1.35 (quintet, J = 7.7 Hz, 2H, the side chain), 1.28−1.12 (m, 8H, 6H of the side chain, 2H of C-ring), 1.08 (s, 3H, 6-Me), 1.03−0.96 (m, 2H, side chain), 0.89−0.82 (m, 1H, C-ring). ^{13}C NMR (100 MHz $CDCl_3$): δ 154.6, 154.5, 149.2, 120.0, 109.5, 108.9, 106.6, 58.0, 50.7, 49.3, 41.6, 38.3, 37.9, 37.6, 35.2, 34.3, 31.0, 29.8 (2 C overlapping), 28.5, 27.9, 27.5, 25.4, 24.9, 23.5, 19.2, 17.2. Mass spectrum (ESI) m/z (relative intensity): 479 (M^+ + H, 100). Exact mass (ESI): calcd for $C_{29}H_{43}N_4O_2$ (M^+ + H), 479.3386; found, 479.3382. HPLC analysis showed a retention time of 5.9 min for the title compound.

*8-(1-((6aR,9R,10aR)-1-Hydroxy-9-(isothiocyanatomethyl)-6,6-dimethyl-6a,7,8,9,10,10a-hexahydro-6H-benzo[c]chromen-3-yl)-cyclopentyl)octanenitrile (**34c**).* To a solution of **33c** (20 mg, 0.04 mmol), in anhydrous THF (0.8 mL) at room temperature, was added triphenyl phosphine (52 mg, 0.2 mmol). Carbon disulfide (70 μL, 1.2 mmol) was then added, and the reaction mixture was stirred for an additional 18 h at the same temperature. Upon completion, the reaction mixture was concentrated under reduced pressure and purified by flash column chromatography on silica gel (10−40% diethyl ether in hexanes) to give 16 mg of **34c** in 78% yield as light-yellow foam. IR (neat): 3394 (OH), 2929, 2858, 2253 (w, CN), 2100 (s, NCS), 1621, 1574, 1451, 1414, 1140, 1037, 838 cm^{-1}; ^1H NMR (500 MHz, $CDCl_3$): δ 6.29 (d, J = 1.8 Hz, 1H, Ar-H), 6.16 (d, J = 1.8 Hz, 1H, Ar-H), 5.06 (br s, 1H, Ar-OH), 3.47 (dd, J = 14.2, 5.4 Hz, 1H, half of an AB system, $-CH_2NCS$), 3.40 (dd, J = 14.2, 6.4 Hz, 1H, half of an AB system, $-CH_2NCS$), 3.25 (m as d, J = 12.6 Hz, 1H of C-ring), 2.47 (m as td, J = 11.2 Hz, J = 2.7 Hz, 1H, C-ring), 2.31 (t, J = 7.1 Hz, 2H, H-8′), 2.02−1.88 (m, 3H, 2H of the cyclopentyl ring, 1H of C-ring), 1.87−1.77 (m, 2H, C-ring), 1.73−1.58 (m, 6H, cyclopentyl ring), 1.55−1.42 (m, 5H, 4H of the side-chain group, 1H of C-ring), 1.39 (s, 3H, 6-Me), 1.34 (quintet, J = 7.7 Hz, 2H, side chain), 1.28−1.12 (m, 8H, 6H of the side chain, 2H of C-ring), 1.08 (s, 3H, 6-Me), 1.03−0.97 (m, 2H, side chain), 0.96−0.87 (m as q, J = 11.9 Hz, 1H, C-ring). ^{13}C NMR (100 MHz $CDCl_3$): δ 154.6, 154.4, 149.3, 130.0, 120.0, 109.2, 109.0, 106.6, 51.2, 50.7, 49.0, 41.6, 38.7, 37.9, 37.6, 35.1, 34.0, 30.6, 29.8, 29.7, 28.5, 27.9, 27.4, 25.4, 24.9, 23.5, 19.2, 17.2. Mass spectrum (ESI) m/z (relative intensity): 495 (M^+ + H, 100). Exact mass (ESI): calcd for $C_{30}H_{43}N_2O_2S$ (M^+ + H), 497.3045; found, 495.3040. HPLC analysis showed a retention time of 6.0 min for the title compound.

Radioligand-Binding Assays. The binding affinities (K_i) of the new compounds were obtained using membrane preparations from rat brain (source of rCB1) or HEK293 cells expressing either mCB2 or hCB2 receptors and [^3H]CP-55,940 as the radioligand, as previously described.[37,38] The results from the competition binding assays were analyzed using nonlinear regression to determine the IC_{50} values for the ligand; K_i values were calculated using the IC_{50} (Prism by GraphPad Software, Inc.). Each experiment was performed in

https://dx.doi.org/10.1021/acs.jmedchem.0c02053
J. Med. Chem. 2021, 64, 3870−3884

triplicate, and K_i values were determined from three independent experiments and are expressed as the mean of these values.

Photoaffinity Covalent Labeling. Rat brain membranes (rCB1, Pel-Freez Biologicals, Rogers, AR) were prepared following the previously described and appropriately modified procedures.[27] Membranes from hCB2 expressed in HEK293 were incubated with the azido ligands in concentrations of 10-fold of their K_i values for 30 min at 37 °C in a water bath with gentle agitation and then exposed to UV (254 nm) for 1 min to activate the ligand.[55] The unbound excess ligand was washed out twice with 1% BSA in TME buffer (25 mM Tris base, 5 mM $MgCl_2$, 1 mM EDTA, pH 7.4). This was followed by an additional washing to remove residual BSA, and the membranes were isolated by centrifugation (Beckman Coulter, JA 20, 17 000 rpm, 10 min, 25 °C). A blank membrane sample was treated in parallel using the same procedure and used as a control.

Electrophilic Covalent Labeling. CB1 and CB2 membranes were incubated with the test ligand in a concentration of 10-fold of their K_i values at 37 °C in a water bath with gentle agitation for 1 h and treated as mentioned above without the photoirradiation step. The unbound excess ligand was washed out twice with 1% BSA in TME and once with TME alone to remove BSA, and the membranes were isolated by centrifugation.

Saturation Binding Assay. Protein concentrations were determined by using a Bio-Rad Bradford protein assay kit,[56] and saturation binding assays were performed in a 96-well format.[30] Membrane pellets were resuspended in TME containing 0.1% BSA. A total of 25 μg of protein was added to each well, and [^{3}H]CP-55,940 was diluted in 0.1% BSA/TME buffer to yield ligand concentrations ranging from 0.5 to 23.8 nM. Nonspecific binding was determined in the presence of 4 μM unlabeled CP-55,940. The assay plates were incubated at 30 °C with gentle agitation for 1 h. The resultant mixture was then transferred to unifilter GF/B filter plates, and the bound ligand was separated from unbound using a Packard Filtermate-96 cell harvester (PerkinElmer Packard, Shelton, CT). Filter plates were washed five times with ice-cold wash buffer (50 mM Tris-base, 5 mM magnesium chloride with 0.5% BSA, pH 7.4). Bound radioactivity was quantitated in a Packard TopCount scintillation counter. Nonspecific binding was subtracted from the total bound radioactivity to calculate the specific binding of [^{3}H]CP-55,940 (measured as pmol/g in saturation curves). Saturation assays were performed in triplicate, and data points were presented as the mean ± SEM. B_{max} and K_d values were calculated by nonlinear regression using GraphPad Prism 4.0 (one-site binding analysis equation $Y = B_{max}X/(K_d + X)$, GraphPad Software, San Diego, CA).

Functional Analysis Studies. The inhibition of forskolin-stimulated cAMP was determined using CISBIO cAMP homogeneous time-resolved fluorescence resonance energy transfer HiRange assay, according to the manufacturer's instructions and as described previously.[8,11] CHO-K1 cells stably expressing 3xHA tagged CB1 or CB2 receptors (3xHA-CB1-CHO or 3xHA-CB2-CHO cells) were plated at 4000 cells per well in white low-volume 384-well plates in Opti-MEM with 1% FBS for 3 h at 37 °C. Cells were then cotreated with 25 μM RO-20-1724 (an inhibitor of phosphodiesterase), 20 μM forskolin (to directly stimulate adenylyl cyclase), and the indicated concentrations of agonists for 30 min at 37 °C. Cells were lysed by the addition of reagents to detect cAMP levels which were incubated at room temperature for 1 h in the dark. Fluorescence was measured at 665 nm/620 nm using a Biotek Synergy Neo Multi-Mode Reader. Data are plotted as the mean ± SEM of four or more experiments performed in duplicate, as noted in the legend. The data were normalized to vehicle and 100 nM CP-55,940 to determine the maximum response (% CP); pharmacological parameters are presented in the tables and were derived from three parameter nonlinear regression curve fitting using GraphPad Prism 8.0.

Molecular Docking. Prediction of ligand binding to CB1 was carried out with Schrodinger Suite 2015−4. Processing of the protein structure (PDB: 5XR8)[8] was performed with the Protein Preparation Wizard. Converting of ligands from 2D to 3D structures was performed using LigPrep. Molecular docking in standard precision was performed with Glide 6.9.[57−59]

Methods for Characterization of *In Vivo* Effects. *Tail-Flick Assay. Subjects.* Male CD-1 mice (n = 6/dose) weighing between 25 and 30 g (Charles River, Wilmington, MA) were used. Mice were housed 4/cage in a climate-controlled vivarium with unrestricted access to food and water. Mice were acclimatized to these vivarium conditions for at least one week before any experimental procedure. Analgesia testing took place at the same time between 9 am and 4 pm. Mice were used once. The experimental protocol for the studies was approved by the Northeastern University Institutional Animal Care and Use Committee. Subjects were maintained in a facility licensed by the Committee on Care and Use of Laboratory Animals of the Institute of Laboratory Animal Resources, National Institutes of Health, 2011.

Drugs. For tail-flick analgesia testing, compound **27a** was initially dissolved in 2% dimethyl sulfoxide, 4% Tween 80, and 4% propylene glycol before saline was slowly added just prior to the 10 mL/kg ip administration. All drug suspensions were prepared just prior to analgesia testing.

Analgesia Procedure. The tail-flick latency test was performed using a thermostatically controlled 2L water bath commercially available from VWR international. The temperature of the water bath for the test day was set at 52 °C. For testing the analgesic effects of compound **27a**, the tip of the tail (2 cm) was immersed in the water bath and withdrawal latency was recorded using a commercially available stopwatch (Fisher Scientific) permitting measurement within 1/100 s. Injections occurred immediately following baseline recording, and five recordings occurred after drug administration at 20, 60, 180, and 360 min, respectively, to complete the analgesia testing. Animals were acclimatized for 3 days prior to the test day (4th day), where tails were immersed in water bath held at room temperature. The tail-flick withdrawal latencies are expressed as a percentage of maximum possible effect (% MPE), based on the formula % MPE = [(test latency minus baseline latency) divided by (10 minus baseline latency)] times 100.

Data Analysis. Nonlinear regression analysis of % MPE data was performed after log-X transformation using Prism Software (v. 5, GraphPad Software, San Diego, CA) to provide estimates of the independent variable when the co-ordinates of X intersected with Y = 50 and their 95% confidence limits (ED_{50} ±95% CL; regression model: log dose or log time *vs* response-variable slope with the top and bottom of the curves constrained to 100 and 0). The results are presented as the mean (±SEM).

Locomotor Assay, Thermoregulation Assay, and Colonic Expulsion Assay. Drugs. WIN 55,212−2 was obtained from Tocris (Tocris, Ellisville, MO, USA). Compound **27a** was synthesized, as described above. All drugs were dissolved in Tween 80 (1%) and DMSO (2%) and then further diluted in 0.9% saline up to the final concentration.

Animals for Behavioral and GI Studies. 9−16 week old male $CB1^{+/+}$ and $CB_1^{-/-}$ mice (25−32 g) on a CB57BL/6 background, as well as 6−8 week old C57BL/6 wild-type mice, were used. The C57BL/6 mice were obtained from Charles River (Montreal, PQ, Canada), and the $CB1^{+/+}$ and $CB_1^{-/-}$ were bred at the University of Calgary mouse breeding facility. Mice were housed at a constant temperature of 22 °C and kept at a constant photoperiod (12:12 h light−dark cycle) in plastic cages on sawdust with access to standard laboratory chow and tap water ad libitum. The mice were used after at least 1 week of acclimation. These experiments were approved by the University of Calgary Animal Care Committee and were performed in accordance with guidelines established by the Canadian Council of Animal Care.

Spontaneous Locomotor Activity Assay. Locomotor activity, assessed in C57Bl/6 mice, was measured using an infrared beam activity monitor (Columbus Instruments, Columbus, OH, USA). Sequential breaking of the invisible infrared beams by the movement of the mouse is recorded, by the monitor, as the ambulatory and horizontal activity counts. Mice were individually placed in the apparatus (at the same location), and the counts were recorded over a 10 min period. The activity apparatus was cleaned with Virkon spray between subjects. Mice underwent a locomotor activity trial in the

https://dx.doi.org/10.1021/acs.jmedchem.0c02053
J. Med. Chem. 2021, 64, 3870−3884

morning (between 9 am and 12 pm) to acclimatize them to the locomotor activity box, and the experiment was conducted in the afternoon (between 1 and 4 pm) of the same day. Mice (n = 6−7/treatment) were injected ip with either **27a** (0.1−1.0 mg/kg), WIN55,122 (1 mg/kg), or vehicle (2% DMSO, 1% Tween 80 in physiological saline). 20 min later, mice were placed in the locomotor activity box where activity was recorded for 10 min.

Thermoregulation Assay. Body temperature was measured using silicone-coated data loggers (SubCue, Calgary, Canada) that were implanted surgically into the abdomen of $CB_1^{-/-}$ and $CB_1^{+/+}$ mice (n = 7−8/treatment) under halothane anesthesia. Following implantation, mice were allowed to recover for 1 week. On day 8−11, mice were injected with **27a** (0.1 mg/kg, ip). Mice were sacrificed 24 h later, and the data logger was removed and data were retrieved and analyzed using SubCue Analyzer software. Core body temperature was taken every 5 min from 6 to 12 days post-implantation, and the data for −100 to 400 post agonist injection were analyzed. The maximum decrease in body temperature from baseline (−100 to 0 min) was determined.

Colonic Expulsion Assay. Distal colonic propulsion was measured, as we have reported previously. After 1-week acclimation, C57BL/7 mice (n = 6−7/treatment) were brought to the laboratory and, following a 1-h acclimation, injected with vehicle (DMSO/Tween 80/saline 2:1:17; ip) or **27a** (0.1 mg/kg ip). After 20, 120, and 220 min, mice were lightly anesthetized with isofluorane and a 2.5 mm glass bead was inserted 2 cm into the rectum with a silicone pusher. Mice were then placed in a glass beaker, and the time to expulsion of the glass bead was monitored. Mice were returned to their home cage between bead insertions. The bead expulsion time of the three trials was determined and reported as the colonic expulsion time in seconds. Data were analyzed by two-way ANOVA with Sidak's multiple comparison.

■ ASSOCIATED CONTENT

Supporting Information

The Supporting Information is available free of charge at https://pubs.acs.org/doi/10.1021/acs.jmedchem.0c02053.

Experimental procedures, spectroscopic, analytical, and physical data for **12a−b**, **13a−b**, **14a−c**, **15a−c**, **16a−c**, **17a−c**, **18a−c**, **19a−c**, **20a−c**, **21a−c**, **22a−c**, **23a−c**, **24a−c**, **25a−c**, **26a−c**, and **27a−c**; saturation binding curves using [^{3}H]CP-55,940 for CB1 and CB2 receptors pre-incubated with the **25a−c**, **26a−c**, **27a−c**, **31c**, **32c**, **33c**, and **34c**; and HPLC traces of **25a**, **26c**, **27b**, and **31c** (PDF).

Molecular formula strings and biochemical data of **25a−c**, **26a−c**, **27a−c**, **31c**, **32c**, **33c**, and **34c** (CSV)

■ AUTHOR INFORMATION

Corresponding Authors

Spyros P. Nikas − *Center for Drug Discovery and Department of Pharmaceutical Sciences, Northeastern University, Boston, Massachusetts 02115, United States;* orcid.org/0000-0001-5052-5292; Phone: +1-617-373-7620; Email: s.nikas@northeastern.edu; Fax: +1-617-373-7493

Alexandros Makriyannis − *Center for Drug Discovery, Department of Pharmaceutical Sciences, and Departments of Chemistry and Chemical Biology, Northeastern University, Boston, Massachusetts 02115, United States;* orcid.org/0000-0003-3272-3687; Phone: +1-617-373-4200; Email: a.makriyannis@northeastern.edu; Fax: +1-617-373-7493

Authors

Shan Jiang − *Center for Drug Discovery and Departments of Chemistry and Chemical Biology, Northeastern University, Boston, Massachusetts 02115, United States*

Christos Iliopoulos-Tsoutsouvas − *Center for Drug Discovery and Department of Pharmaceutical Sciences, Northeastern University, Boston, Massachusetts 02115, United States*

Fei Tong − *Center for Drug Discovery and Department of Pharmaceutical Sciences, Northeastern University, Boston, Massachusetts 02115, United States*

Christina A. Brust − *Department of Molecular Medicine, The Scripps Research Institute, Jupiter, Florida 33458, United States*

Catherine M. Keenan − *Hotchkiss Brain Institute and Snyder Institute for Chronic Diseases, Department of Physiology and Pharmacology, University of Calgary, Calgary, Alberta T2N 4N1, Canada*

Jimit Girish Raghav − *Center for Drug Discovery and Department of Pharmaceutical Sciences, Northeastern University, Boston, Massachusetts 02115, United States*

Tian Hua − *iHuman Institute, ShanghaiTech University, Shanghai 201210, China*

Simiao Wu − *Center for Drug Discovery and Department of Pharmaceutical Sciences, Northeastern University, Boston, Massachusetts 02115, United States*

Jo-Hao Ho − *Department of Molecular Medicine, The Scripps Research Institute, Jupiter, Florida 33458, United States*

Yiran Wu − *iHuman Institute, ShanghaiTech University, Shanghai 201210, China*

Travis W. Grim − *Department of Molecular Medicine, The Scripps Research Institute, Jupiter, Florida 33458, United States*

Nikolai Zvonok − *Center for Drug Discovery and Department of Pharmaceutical Sciences, Northeastern University, Boston, Massachusetts 02115, United States*

Ganesh A. Thakur − *Center for Drug Discovery and Department of Pharmaceutical Sciences, Northeastern University, Boston, Massachusetts 02115, United States;* orcid.org/0000-0002-7468-8819

Zhi-Jie Liu − *iHuman Institute, ShanghaiTech University, Shanghai 201210, China*

Keith A. Sharkey − *Hotchkiss Brain Institute and Snyder Institute for Chronic Diseases, Department of Physiology and Pharmacology, University of Calgary, Calgary, Alberta T2N 4N1, Canada*

Laura M. Bohn − *Department of Molecular Medicine, The Scripps Research Institute, Jupiter, Florida 33458, United States*

Complete contact information is available at: https://pubs.acs.org/10.1021/acs.jmedchem.0c02053

Author Contributions

#S.J. and C.I.-T. contributed equally

Notes

The authors declare no competing financial interest.

■ ACKNOWLEDGMENTS

This work was supported by grants from the National Institute on Drug Abuse to A.M. (DA026795, DA041435, DA045020 DA009158, and DA007215) and from the Canadian Institutes of Health Research to K.A.S. K.A.S. holds the Crohn's and

Colitis Canada Chair in Inflammatory Bowel Disease Research at the University of Calgary.

■ ABBREVIATIONS

BSA, bovine serum albumin; cAMP, 3′,5′-cyclic adenosine monophosphate; CHO, Chinese hamster ovary cell line; (−)-Δ^9-THC, (−)-Δ^9-tetrahydrocannabinol; DIBAL-H, diisobutylaluminum hydride; DMAP, *N*,*N*-dimethyl-4-aminopyridine; DMF, *N*,*N*-dimethylformamide; DMSO, dimethylsulfoxide; ESI, electron spray ionization; GPCR, G protein-coupled receptor; HHC, hexahydrocannabinol; HEK293, human embryonic kidney cell line; KHMDS, potassium bis(trimethylsilyl)amide; LAPS, ligand assisted protein structure; MPE, maximum possible effect; NMR, nuclear magnetic resonance; rt, room temperature; SEM, standard error of mean; TBSCl, *tert*-butyldimethylsilyl chloride; TBAF, tetra-*n*-butylammonium fluoride; THC, tetrahydrocannabinol; THF, tetrahydrofuran; TMG-N_3, *N*,*N*,*N*′,*N*′-tetramethylguanidinium azide; TMS, tetramethylsilane; TMSOTf, trimethylsilyl trifluoromethanesulfonate

■ REFERENCES

(1) Cristino, L.; Bisogno, T.; Di Marzo, V. Cannabinoids and the expanded endocannabinoid system in neurological disorders. *Nat. Rev. Neurol.* **2020**, *16*, 9−29.

(2) Janero, D. R.; Makriyannis, A. Cannabinoid receptor antagonists: pharmacological opportunities, clinical experience, and translational prognosis. *Expert Opin. Emerging Drugs* **2009**, *14*, 43−65.

(3) Cairns, E. A.; Baldridge, W. H.; Kelly, M. E. The endocannabinoid system as a therapeutic target in glaucoma. *Neural Plast.* **2016**, *2016*, 9364091.

(4) Woodhams, S. G.; Chapman, V.; Finn, D. P.; Hohmann, A. G.; Neugebauer, V. The cannabinoid system and pain. *Neuropharmacology* **2017**, *124*, 105−120.

(5) Hinz, B.; Ramer, R. Anti-tumour actions of cannabinoids. *Br. J. Pharmacol.* **2019**, *176*, 1384−1394.

(6) Turcotte, C.; Blanchet, M.-R.; Laviolette, M.; Flamand, N. The CB2 receptor and its role as a regulator of inflammation. *Cell. Mol. Life Sci.* **2016**, *73*, 4449−4470.

(7) Thakur, G. A.; Nikas, S. P.; Li, C.; Makriyannis, A. Structural requirements for cannabinoid receptor probes. *Handb. Exp. Pharmacol.* **2005**, *168*, 209−246.

(8) Hua, T.; Vemuri, K.; Nikas, S. P.; Laprairie, R. B.; Wu, Y.; Qu, L.; Pu, M.; Korde, A.; Jiang, S.; Ho, J.-H.; Han, G. W.; Ding, K.; Li, X.; Liu, H.; Hanson, M. A.; Zhao, S.; Bohn, L. M.; Makriyannis, A.; Stevens, R. C.; Liu, Z.-J. Crystal structures of agonist-bound human cannabinoid receptor CB1. *Nature* **2017**, *547*, 468−471.

(9) Hua, T.; Vemuri, K.; Pu, M.; Qu, L.; Han, G. W.; Wu, Y.; Zhao, S.; Shui, W.; Li, S.; Korde, A.; Laprairie, R. B.; Stahl, E. L.; Ho, J.-H.; Zvonok, N.; Zhou, H.; Kufareva, I.; Wu, B.; Zhao, Q.; Hanson, M. A.; Bohn, L. M.; Makriyannis, A.; Stevens, R. C.; Liu, Z.-J. Crystal Structure of the Human Cannabinoid Receptor CB1. *Cell* **2016**, *167*, 750−762.

(10) Krishna Kumar, K.; Shalev-Benami, M.; Robertson, M. J.; Hu, H.; Banister, S. D.; Hollingsworth, S. A.; Latorraca, N. R.; Kato, H. E.; Hilger, D.; Maeda, S.; Weis, W. I.; Farrens, D. L.; Dror, R. O.; Malhotra, S. V.; Kobilka, B. K.; Skiniotis, G. Structure of a signaling cannabinoid receptor 1-G protein complex. *Cell* **2019**, *176*, 448−458.

(11) Hua, T.; Li, X.; Wu, L.; Iliopoulos-Tsoutsouvas, C.; Wang, Y.; Wu, M.; Shen, L.; Johnston, C. A.; Nikas, S. P.; Song, F.; Song, X.; Yuan, S.; Sun, Q.; Wu, Y.; Jiang, S.; Grim, T. W.; Benchama, O.; Stahl, E. L.; Zvonok, N.; Zhao, S.; Bohn, L. M.; Makriyannis, A.; Liu, Z.-J. Activation and signaling mechanism revealed by cannabinoid receptor-Gi complex structures. *Cell* **2020**, *180*, 655−665.

(12) Khajehali, E.; Malone, D. T.; Glass, M.; Sexton, P. M.; Christopoulos, A.; Leach, K. Biased agonism and biased allosteric modulation at the CB1 cannabinoid receptor. *Mol. Pharmacol.* **2015**, *88*, 368−379.

(13) Mallipeddi, S.; Janero, D. R.; Zvonok, N.; Makriyannis, A. Functional selectivity at G-protein coupled receptors: Advancing cannabinoid receptors as drug targets. *Biochem. Pharmacol.* **2017**, *128*, 1−11.

(14) Rankovic, Z.; Brust, T. F.; Bohn, L. M. Biased agonism: An emerging paradigm in GPCR drug discovery. *Bioorg. Med. Chem. Lett.* **2016**, *26*, 241−250.

(15) Tan, L.; Yan, W.; McCorvy, J. D.; Cheng, J. Biased Ligands of G Protein-Coupled Receptors (GPCRs): Structure−Functional Selectivity Relationships (SFSRs) and Therapeutic Potential. *J. Med. Chem.* **2018**, *61*, 9841−9878.

(16) Guo, D.; Hillger, J. M.; IJzerman, A. P.; Heitman, L. H. Drug-target residence time−a case for G protein-coupled receptors. *Med. Res. Rev.* **2014**, *34*, 856−892.

(17) van der Velden, W. J. C.; Heitman, L. H.; Rosenkilde, M. M. Perspective: Implications of ligand-receptor binding kinetics for therapeutic targeting of G protein-coupled receptors. *ACS Pharmacol. Transl. Sci.* **2020**, *3*, 179−189.

(18) Swinney, D.; Haubrich, B.; Liefde, I.; Vauquelin, G. The role of binding kinetics in GPCR drug discovery. *Curr. Top. Med. Chem.* **2015**, *15*, 2504−2522.

(19) Keenan, C. M.; Storr, M. A.; Thakur, G. A.; Wood, J. T.; Wager-Miller, J.; Straiker, A.; Eno, M. R.; Nikas, S. P.; Bashashati, M.; Hu, H.; Mackie, K.; Makriyannis, A.; Sharkey, K. A. AM841, a covalent cannabinoid ligand, powerfully slows gastrointestinal motility in normal and stressed mice in a peripherally restricted manner. *Br. J. Pharmacol.* **2015**, *172*, 2406−2418.

(20) Szymanski, D. W.; Papanastasiou, M.; Melchior, K.; Zvonok, N.; Mercier, R. W.; Janero, D. R.; Thakur, G. A.; Cha, S.; Wu, B.; Karger, B.; Makriyannis, A. Mass spectrometry-based proteomics of human cannabinoid receptor 2: covalent cysteine 6.47(257)-ligand interaction affording megagonist receptor activation. *J. Proteome Res.* **2011**, *10*, 4789−4798.

(21) Herenbrink, C. K.; Sykes, D. A.; Donthamsetti, P.; Canals, M.; Coudrat, T.; Shonberg, J.; Scammells, P. J.; Capuano, B.; Sexton, P. M.; Charlton, S. J.; Javitch, J. A.; Christopoulos, A.; Lane, J. R. The role of kinetic context in apparent biased agonism at GPCRs. *Nat. Commun.* **2016**, *7*, 10842.

(22) Makriyannis, A. 2012 Division of medicinal chemistry award address. Trekking the cannabinoid road: a personal perspective. *J. Med. Chem.* **2014**, *57*, 3891−3911.

(23) Janero, D. R.; Korde, A.; Makriyannis, A. Ligand-Assisted Protein Structure (LAPS): An Experimental Paradigm for Characterizing Cannabinoid-Receptor Ligand-Binding Domains. *Methods Enzymol.* **2017**, *593*, 217−235.

(24) Janero, D. R.; Yaddanapudi, S.; Zvonok, N.; Subramanian, K. V.; Shukla, V. G.; Stahl, E.; Zhou, L.; Hurst, D.; Wager-Miller, J.; Bohn, L. M.; Reggio, P. H.; Mackie, K.; Makriyannis, A. Molecular-interaction and signaling profiles of AM3677, a novel covalent agonist selective for the cannabinoid 1 receptor. *ACS Chem. Neurosci.* **2015**, *6*, 1400−1410.

(25) Chu, C.; Ramamurthy, A.; Makriyannis, A.; Tius, M. A. Synthesis of covalent probes for the radiolabeling of the cannabinoid receptor. *J. Org. Chem.* **2003**, *68*, 55−61.

(26) Li, C.; Xu, W.; Vadivel, S. K.; Fan, P.; Makriyannis, A. High affinity electrophilic and photoactivatable covalent endocannabinoid probes for the CB1 receptor. *J. Med. Chem.* **2005**, *48*, 6423−6429.

(27) Ogawa, G.; Tius, M. A.; Zhou, H.; Nikas, S. P.; Halikhedkar, A.; Mallipeddi, S.; Makriyannis, A. 3'-functionalized adamantyl cannabinoid receptor probes. *J. Med. Chem.* **2015**, *58*, 3104−3116.

(28) Zhou, H.; Peng, Y.; Halikhedkar, A.; Fan, P.; Janero, D. R.; Thakur, G. A.; Mercier, R. W.; Sun, X.; Ma, X.; Makriyannis, A. Human cannabinoid receptor 2 ligand-interaction motif: Transmembrane helix 2 cysteine, C2.59(89), as determinant of classical cannabinoid agonist activity and binding pose. *ACS Chem. Neurosci.* **2017**, *8*, 1338−1347.

https://dx.doi.org/10.1021/acs.jmedchem.0c02053
J. Med. Chem. 2021, 64, 3870−3884

(29) Szymanski, D.; Papanastasiou, M.; Pandarinathan, L.; Zvonok, N.; Janero, D. R.; Pavlopoulos, S.; Vouros, P.; Makriyannis, A. Aliphatic Azides as Selective Cysteine Labeling Reagents for Integral Membrane Proteins. *J. Med. Chem.* **2018**, *61*, 11199−11208.
(30) Picone, R. P.; Khanolkar, A. D.; Xu, W.; Ayotte, L. A.; Thakur, G. A.; Hurst, D. P.; Abood, M. E.; Reggio, P. H.; Fournier, D. J.; Makriyannis, A. (-)-7′-Isothiocyanato-11-hydroxy-1′, 1′-dimethylheptylhexahydrocannabinol (AM841), a high-affinity electrophilic ligand, interacts covalently with a cysteine in helix six and activates the CB1 cannabinoid receptor. *Mol. Pharmacol.* **2005**, *68*, 1623−1635.
(31) Pei, Y.; Mercier, R. W.; Anday, J. K.; Thakur, G. A.; Zvonok, A. M.; Hurst, D.; Reggio, P. H.; Janero, D. R.; Makriyannis, A. Ligand-binding architecture of human CB2 cannabinoid receptor: evidence for receptor subtype-specific binding motif and modeling GPCR activation. *Chem. Biol.* **2008**, *15*, 1207−1219.
(32) Mercier, R. W.; Pei, Y.; Pandarinathan, L.; Janero, D. R.; Zhang, J.; Makriyannis, A. hCB2 ligand-interaction landscape: cysteine residues critical to biarylpyrazole antagonist binding motif and receptor modulation. *Chem. Biol.* **2010**, *17*, 1132−1142.
(33) Mallipeddi, S.; Kreimer, S.; Zvonok, N.; Vemuri, K.; Karger, B. L.; Ivanov, A. R.; Makriyannis, A. Binding site characterization of AM1336, a novel covalent inverse agonist at human cannabinoid 2 receptor, using mass spectrometric analysis. *J. Proteome Res.* **2017**, *16*, 2419−2428.
(34) Thakur, G.; Nikas, S.; Makriyannis, A. CB1 cannabinoid receptor ligands. *Mini-Rev. Med. Chem.* **2005**, *5*, 631−640.
(35) Papahatjis, D. P.; Nikas, S. P.; Kourouli, T.; Chari, R.; Xu, W.; Pertwee, R. G.; Makriyannis, A. Pharmacophoric requirements for the cannabinoid side chain. Probing the cannabinoid receptor subsite at C1′. *J. Med. Chem.* **2003**, *46*, 3221−3229.
(36) Papahatjis, D. P.; Nahmias, V. R.; Nikas, S. P.; Andreou, T.; Alapafuja, S. O.; Tsotinis, A.; Guo, J.; Fan, P.; Makriyannis, A. C1 ‘-cycloalkyl side chain pharmacophore in tetrahydrocannabinols. *J. Med. Chem.* **2007**, *50*, 4048−4060.
(37) Nikas, S. P.; Alapafuja, S. O.; Papanastasiou, I.; Paronis, C. A.; Shukla, V. G.; Papahatjis, D. P.; Bowman, A. L.; Halikhedkar, A.; Han, X.; Makriyannis, A. Novel 1’,1’-chain substituted hexahydrocannabinols: 9beta-hydroxy-3-(1-hexyl-cyclobut-1-yl)-hexahydrocannabinol (AM2389) a highly potent cannabinoid receptor 1 (CB1) agonist. *J. Med. Chem.* **2010**, *53*, 6996−7010.
(38) Nikas, S. P.; Sharma, R.; Paronis, C. A.; Kulkarni, S.; Thakur, G. A.; Hurst, D.; Wood, J. T.; Gifford, R. S.; Rajarshi, G.; Liu, Y.; Raghav, J. G.; Guo, J. J.; Järbe, T. U. C.; Reggio, P. H.; Bergman, J.; Makriyannis, A. Probing the carboxyester side chain in controlled deactivation (-)-delta(8)-tetrahydrocannabinols. *J. Med. Chem.* **2015**, *58*, 665−681.
(39) Nikas, S. P.; Grzybowska, J.; Papahatjis, D. P.; Charalambous, A.; Banijamali, A. R.; Chari, R.; Fan, P.; Kourouli, T.; Lin, S.; Nitowski, A. J.; Marciniak, G.; Guo, Y.; Li, X.; Wang, C.-L. J.; Makriyannis, A. The role of halogen substitution in classical cannabinoids: a CB1 pharmacophore model. *AAPS J.* **2004**, *6*, 23−35.
(40) Bow, E. W.; Rimoldi, J. M. The Structure−Function Relationships of Classical Cannabinoids: CB1/CB2 Modulation. *Perspect. Med. Chem.* **2016**, *8*, 17−39.
(41) Busch-Petersen, J.; Hill, W. A.; Fan, P.; Khanolkar, A.; Xie, X.-Q.; Tius, M. A.; Makriyannis, A. Unsaturated side chain beta-11-hydroxyhexahydrocannabinol analogs. *J. Med. Chem.* **1996**, *39*, 3790−3796.
(42) Makriyannis, A.; Pavlopoulos, S.; Thakur, G. A.; Nikas, S. P. Cannabinoid receptors as therapeutic targets. *Curr. Pharm. Des.* **2006**, *12*, 1751−1769.
(43) Drake, D. J.; Jensen, R. S.; Busch-Petersen, J.; Kawakami, J. K.; Concepcion Fernandez-Garcia, M.; Fan, P.; Makriyannis, A.; Tius, M. A. Classical/nonclassical hybrid cannabinoids: southern aliphatic chain-functionalized C-6β methyl, ethyl, and propyl analogues. *J. Med. Chem.* **1998**, *41*, 3596−3608.
(44) Kulkarni, S.; Nikas, S. P.; Sharma, R.; Jiang, S.; Paronis, C. A.; Leonard, M. Z.; Zhang, B.; Honrao, C.; Mallipeddi, S.; Raghav, J. G.; Benchama, O.; Järbe, T. U. C.; Bergman, J.; Makriyannis, A. Novel C-Ring-Hydroxy-Substituted Controlled Deactivation Cannabinergic Analogues. *J. Med. Chem.* **2016**, *59*, 6903−6919.
(45) Fleming, F. F.; Yao, L.; Ravikumar, P. C.; Funk, L.; Shook, B. C. Nitrile-containing pharmaceuticals: efficacious roles of the nitrile pharmacophore. *J. Med. Chem.* **2010**, *53*, 7902−7917.
(46) Sharma, R.; Nikas, S. P.; Paronis, C. A.; Wood, J. T.; Halikhedkar, A.; Guo, J. J.; Thakur, G. A.; Kulkarni, S.; Benchama, O.; Raghav, J. G.; Gifford, R. S.; Järbe, T. U. C.; Bergman, J.; Makriyannis, A. Controlled-deactivation cannabinergic ligands. *J. Med. Chem.* **2013**, *56*, 10142−10157.
(47) Archer, R. A.; Blanchard, W. B.; Day, W. A.; Johnson, D. W.; Lavagnino, E. R.; Ryan, C. W.; Baldwin, J. E. Cannabinoids. 3. Synthetic approaches to 9-ketocannabinoids. Total synthesis of nabilone. *J. Org. Chem.* **1977**, *42*, 2277−2284.
(48) Nikas, S. P.; Thakur, G. A.; Parrish, D.; Alapafuja, S. O.; Huestis, M. A.; Makriyannis, A. A concise methodology for the synthesis of (−)-Δ9-tetrahydrocannabinol and (−)-Δ9-tetrahydrocannabivarin metabolites and their regiospecifically deuterated analogs. *Tetrahedron* **2007**, *63*, 8112−8123.
(49) Peyrat, J.-F.; Figadère, B.; Cavé, A. Halide exchange: Preparation of alkyl chlorides. *Synth. Commun.* **1996**, *26*, 4563−4567.
(50) Guo, Y.; Abadji, V.; Morse, K. L.; Fournier, D. J.; Li, X.; Makriyannis, A. (-)-11-Hydroxy-7’-isothiocyanato-1’, 1’-dimethylheptyl-. DELTA. 8-THC: A Novel, High-Affinity Irreversible Probe for the Cannabinoid Receptor in the Brain. *J. Med. Chem.* **1994**, *37*, 3867−3870.
(51) Khanolkar, A. D.; Lu, D.; Ibrahim, M.; Duclos, R. I., Jr.; Thakur, G. A.; Malan, T. P., Jr.; Porreca, F.; Veerappan, V.; Tian, X.; George, C.; Parrish, D. A.; Papahatjis, D. P.; Makriyannis, A. Cannabilactones: a novel class of CB2 selective agonists with peripheral analgesic activity. *J. Med. Chem.* **2007**, *50*, 6493−6500.
(52) Li, X.; Hua, T.; Vemuri, K.; Ho, J.-H.; Wu, Y.; Wu, L.; Popov, P.; Benchama, O.; Zvonok, N.; Locke, K. a.; Qu, L.; Han, G. W.; Iyer, M. R.; Cinar, R.; Coffey, N. J.; Wang, J.; Wu, M.; Katritch, V.; Zhao, S.; Kunos, G.; Bohn, L. M.; Makriyannis, A.; Stevens, R. C.; Liu, Z.-J. Crystal Structure of the Human Cannabinoid Receptor CB2. *Cell* **2019**, *176*, 459−467.
(53) Ballesteros, J. A.; Weinstein, H. Integrated methods for the construction of three-dimensional models and computational probing of structure-function relations in G protein-coupled receptors. *Methods Neurosci.* **1995**, *25*, 366−428.
(54) Little, P. J.; Compton, D. R.; Johnson, M. R.; Melvin, L. S.; Martin, B. R. Pharmacology and stereoselectivity of structurally novel cannabinoids in mice. *J. Pharmacol. Exp. Ther.* **1988**, *247*, 1046−1051.
(55) Cavalla, D.; Neff, N. H. Chemical mechanisms for photoaffinity labeling of receptors. *Biochem. Pharmacol.* **1985**, *34*, 2821−2826.
(56) Braford, M. M. A rapid and sensitive method for the quantification of microgram quantities of protein utilizing the principle of protein-dye banding. *Anal. Biochem.* **1976**, *72*, 248−254.
(57) Friesner, R. A.; Banks, J. L.; Murphy, R. B.; Halgren, T. A.; Klicic, J. J.; Mainz, D. T.; Repasky, M. P.; Knoll, E. H.; Shelley, M.; Perry, J. K.; Shaw, D. E.; Francis, P.; Shenkin, P. S. Glide: a new approach for rapid, accurate docking and scoring. 1. Method and assessment of docking accuracy. *J. Med. Chem.* **2004**, *47*, 1739−1749.
(58) Halgren, T. A.; Murphy, R. B.; Friesner, R. A.; Beard, H. S.; Frye, L. L.; Pollard, W. T.; Banks, J. L. Glide: a new approach for rapid, accurate docking and scoring. 2. Enrichment factors in database screening. *J. Med. Chem.* **2004**, *47*, 1750−1759.
(59) Friesner, R. A.; Murphy, R. B.; Repasky, M. P.; Frye, L. L.; Greenwood, J. R.; Halgren, T. A.; Sanschagrin, P. C.; Mainz, D. T. Extra precision glide: docking and scoring incorporating a model of hydrophobic enclosure for protein-ligand complexes. *J. Med. Chem.* **2006**, *49*, 6177−6196.

https://dx.doi.org/10.1021/acs.jmedchem.0c02053
J. Med. Chem. 2021, 64, 3870−3884